Prog. Energy Combust. Sci., Vol. 6, pp. 303–329.
Pergamon Press Ltd., 1980. Printed in Great Britain.

0360-1285/80/1201-0303$05.00/0

THE DETERMINATION OF LAMINAR BURNING VELOCITY

C. J. RALLIS and A. M. GARFORTH
School of Mechanical Engineering, University of the Witwatersrand, Jan Smuts Avenue, Johannesburg 2001, South Africa

Abstract—The relevance of data on laminar burning velocities, both from their value to industry and related research areas, and for the validation of theoretical chemical kinetic models, is discussed, as are certain fundamental problems associated with the measurement of this intrinsic property. Various methods which have been used over the years to experimentally determine this property are reviewed and it is concluded that the spherical constant-volume vessel method is both the most versatile and accurate. As a consequence, a summary of the equations required for its correct use are presented. For the purpose of comparing the results of the more reliable techniques, as well as comparing these with recent computer predictions, data on the effects of equivalence ratio, pressure and unburnt gas temperature for methane–air mixtures are reported, as are a number of empirical equations correlating these variables with burning velocity.

NOTATION

A area;
B defined as $(1/\beta)(\bar{\varepsilon} - \bar{\alpha})(1 - F^2)$;
C defined as $-(1/\beta)(r_f/3)(1 - F^3)$, specific heat capacity;
D defined as $-C$, diffusion coefficient;
E defined as $BF^2/(1 - F^2)$;
F defined as $(1 - \tilde{r})$;
G defined as $\bar{\alpha}F^3 + \bar{\varepsilon}(1 - F^3)$;
h enthalpy;
k constant;
K correction factor;
m mass;
M molecular weight;
n mass fraction;
p absolute pressure;
r radius;
R bomb inner-wall radius, tube radius;
R universal gas constant;
S velocity;
t time;
T absolute temperature;
v velocity;
W reaction rate;
x distance;
y distance;
α defined as (ρ_b/ρ_o), angle;
β defined as (ρ_w/ρ_o);
γ ratio of heat capacities;
ε defined as (ρ_f/ρ_o);
ρ density;
τ flame-front thickness;
ϕ equivalence ratio;

Subscripts
b burnt gas;
c centre, correction;
e at end of combustion;
f flame front;
i ignition;
λ thermal conductivity;
o initial;
p constant pressure;
pr preheat zone;
s spatial;
t transformation (or burning), throat;
u unburnt gas;
ug unburnt gas;
w at the bomb wall;

A bar over any symbol indicates an instantaneously spatially-averaged value. The symbol ˜ denotes nondimensional quantities.

1. INTRODUCTION

The main aim of combustion research is the acquisition of a thorough understanding of the mechanisms of ignition, species distribution, flame propagation and energy release of combustible mixtures. The practical results of such knowledge are evidently the control of the combustion process, both from the point of view of safety and its utilization as a source of energy.

Ultimately, such understanding can only be achieved through chemical kinetics—the mass, species and energy equations being used to predict the conditions necessary for ignition, as well as the overall rates of reaction (HC53, HC54, Sp56). Unfortunately, due to the complexity of the problem, this method has only recently started yielding results, and then only for the simpler combustible mixtures (SH76, Ts78). In any event, the validation of any theoretical model requires the availability of reliable experimental data against which its prediction can be compared (SH76, HK77, Ts78).

The proximate goal of gradually accumulating knowledge via *ad hoc* experimentation is thus still necessary—both in the short and long terms. Furthermore, correlation of such data can provide valuable clues for elucidation by more comprehensive theoretical treatments. To quote Lewis (Le59), ". . . it is possible to develop new conceptional understandings from experimental observations and simple correlations whenever it is found that flame processes have some physical basis in common".

Two complementary empirical approaches to the study of combustion processes are available—microscopic and macroscopic. The aim of the former, which use measuring instruments of high spatial resolution and short response time, is to provide

detailed descriptions of flame structure through information of the fluid flow, temperature and composition profiles, reaction rates and transport coefficients of the various species present in the flame (Go76). The latter provide data on the effects of thermodynamic variables such as composition, temperature, and pressure, on the gross behavior of combustible mixtures: *viz.* inflammability limits; ignition energies, temperatures, and delays; quenching distances; instability phenomena; burning velocities of both laminar and turbulent flames; abnormal combustion such as detonation and knock; and the like.

This review will be primarily concerned with the experimental determination of one of the basic properties of any combustible mixture—its laminar burning velocity.

A number of excellent reviews have been published over the years on this topic. Notable amongst these are those of Lewis and von Elbe (LV56, LV61), Linnett (Li53, Li54), Fiock (Fi43, Fi55), Simon and Wong (SW53), Dugger *et al.* (DS57), Gaydon and Wolfhard (GW60), Laffite and Combourieu (La62, Co62 and LC64), Fristrom and Westenberg (FW65), Lidlow (Li67) and, more recently, of Andrews and Bradley (AB72).

What is perhaps surprising is that although the subject of the burning velocity of combustible mixtures has been studied for close on a century, there is still a lack of consensus both as to the most effective methods of measurement and on the reliability of the published data for various mixtures.

2. FLAME-FRONT STRUCTURE

As a prerequisite to the reliable determination of burning velocity it is necessary to have some understanding of flame-front structure.

A flame is the result of a self-sustaining chemical reaction usually made visible by the luminosity of the burning gases. Associated with a flame is a flame front, in which the unburnt gas is heated and converted into products. Whether the flame is stationary or moving in space, the flame front, which is of finite thickness, is taken as an indication of the progress of the flame.

The flame front is generally considered to consist of two regions, referred to as the preheat and reaction zones (Fig. 1).

The preheat zone occurs between the cold boundary, at temperature, T_u, and the location of the ignition temperature, T_i. In this region, the temperature of the unburnt gas is raised mainly by heat conduction and some convection from the reaction zone—radiation heat transfer being negligible. Since each element in this region acts as a heat sink, the temperature profile is concave upwards ($\partial^2 T/\partial x^2 > 0$). Also, because of the temperature increase, the unburnt gas expands and is accelerated (Fig. 2). No significant chemical reaction occurs in this zone (DS57).

On reaching its ignition temperature, T_i, each element of gas starts undergoing chemical reaction with a consequent evolution of heat, resulting in a temperature profile which is concave downwards ($\partial^2 T/\partial x^2 < 0$). The temperature continues to rise until its equilibrium value of T_f is reached. The region between the location of the ignition temperature, T_i, and the hot boundary at the equilibrium temperature, T_f, is referred to as the reaction zone (Fig. 1).

The reaction zone is further divisible into two parts: the primary and secondary reaction zones. The primary zone is approximately coincident with the luminous zone (WF61), while the secondary zone is associated with an area of weak secondary luminosity due to CO oxidation (FW65).

The whole region comprising the preheat and reaction zones—characterized by the term flame front—generally has a significant thickness. Ideally, this thickness is the distance between the cold and hot boundaries of the front. However, since the temperature profile approaches both T_u and T_f asymptotically, its extremities are usually specified by the arbitrary conditions:

$$(T_i - T_u')/(T_i - T_u) = 0.99$$
$$(T_f' - T_i)/(T_f - T_i) = 0.99 \qquad (1)$$

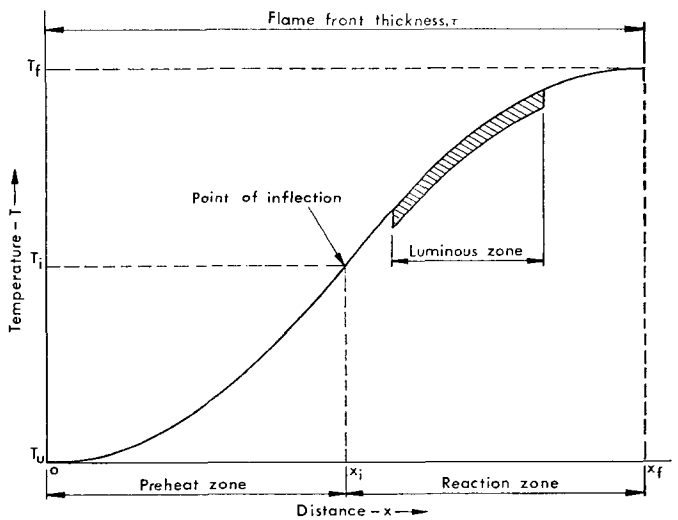

FIG. 1. Typical temperature profile through a flame front.

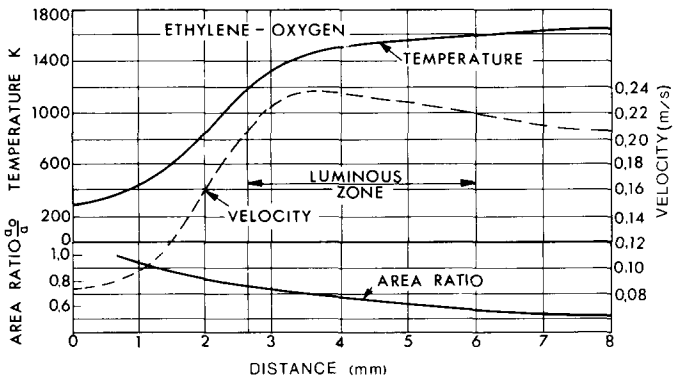

FIG. 2. Temperature, velocity, and stream-tube area profiles (Fr61).

where T_u' and T_f' are the temperatures at these arbitrary extremes.

Application of eq. (1) to the temperature distribution through the preheat zone via the conservation equations presented in Section 3 yields an estimate of the thickness of this zone, given by

$$\tau_{pr} = 4.6\bar{\lambda}/\bar{C}_p\rho_u S_t. \tag{2}$$

Evidently (FW65), this relationship is representative of a total flame thickness, τ', defined in terms of the average temperature gradient through the front, as indicated in Fig. 3.

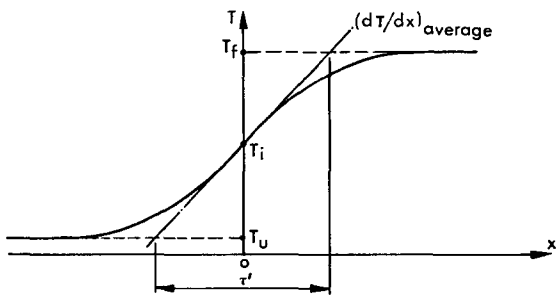

FIG. 3. Flame-front thickness based on preheat zone analysis.

The foregoing description is relevant in this review for two reasons. As will be discussed in Section 4, the determination of burning velocity in experiments in which the flame front is not plane, is critically dependent on the decision taken regarding the location of this front (Li53). Also, since at low densities (ρ_u) and burning velocities (S_t) the thickness of the flame front can become significant, this effect must be incorporated into the equations used to calculate burning velocity (Section 7.2).

As with temperature and velocity, species concentration profiles also exist within the flame front (Fig. 4). The latter are much more complex than either the temperature or velocity profiles, and are largely dependent upon the combustible mixture concerned. These profiles are not of direct relevance in this review provided that, at any stage through the flame, the system may be considered as a mixture of perfect gases for the purposes of density calculation.

The interested reader is referred to the literature for more detailed treatments of flame structure (Fr61, FW65).

3. CONSERVATION EQUATIONS FOR A PROPAGATING FLAME-FRONT

Two main methods for calculating laminar burning velocity and flame structure have been evolved during the past three decades. The ordinary differential equations for heat conduction, diffusion and species continuity derived by Hirschfelder *et al.* (HC53) and solved by them by the simple shooting method represents one approach. Here, the flame speed is the eigenvalue of the two-point boundary value problem specified by the unburnt and burnt gas conditions. Often, however, an assumed burning velocity is not sufficient to initiate the solution, and multi-eigenvalue solutions are necessary (CH63). No acceptable convergence criteria exist for such solutions and, although other methods have been devised (Ke68), no standardization has been achieved.

The other main approach, used by Spalding (Sp56), involves setting up the equations for continuity and the time-dependent energy conservation equations. These are solved by finite-difference methods, with arbitrary initial profile assumptions. They are more easily applied to the unsteady propagation of laminar flames than are those of Hirschfelder *et al.* As used by Adams and Cook (AC60), Zeldovich and Barenblatt (ZB59), Dixon-Lewis (DL67) and Spalding *et al.* (SS71), these equations have been applied to the solution of the one-dimensional flame problem. Recently, the method has been extended to handle flames in cylindrical and spherical co-ordinates by Bledjian (B173) and Dixon-Lewis and Shepherd (DS74).

Pertinent recent references covering the procedures and problems encountered include DS74, DG75, SH76 and Ts78.

In this form the equations are only applicable to the adiabatic flame case. These equations are:

(1) The *mass continuity* equation—

$$(\partial\rho/\partial t) + (1/r^k)(\partial/\partial r)(r^k\rho v) = 0. \tag{3}$$

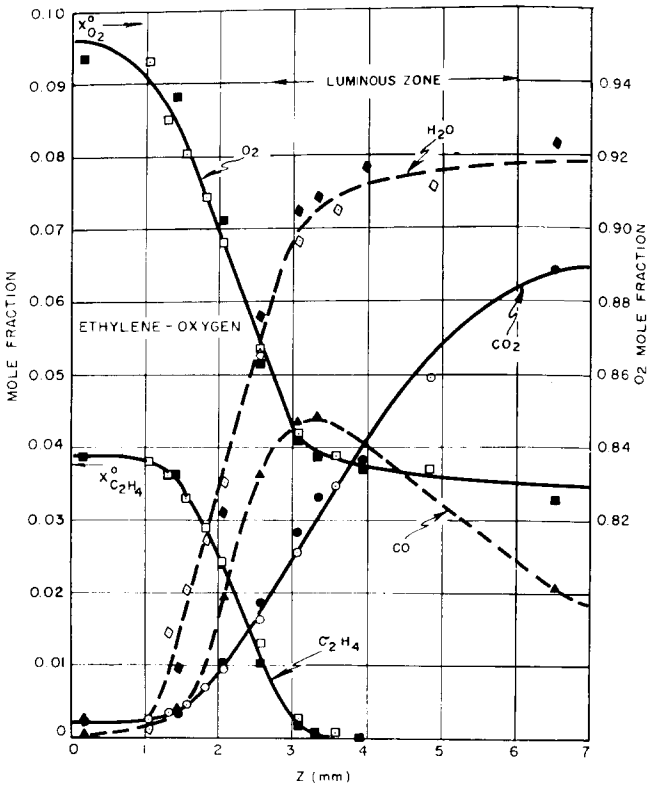

FIG. 4. Composition profiles of lean ethylene–oxygen flame (Fr61).

(2) The *species continuity* equation—

$$(\partial y_i/\partial t) + v(\partial y_i/\partial r) = (1/\rho r^k)(\partial/\partial r)[r^k D_i \rho(\partial y_i/\partial r)] + W_i \rho. \quad (4)$$

(3) The *energy conservation* equation, in terms of static temperature—

$$C_p(\partial T/\partial t) + vC_p(\partial T/\partial r) = (1/\rho r^k)(\partial/\partial r)[r^k \lambda(\partial T/\partial r)] - \sum_{i=1}^{n} (W_i h_i/\rho) + \sum_{i=1}^{n} D_i(\partial y_i/\partial r)(\partial h_i/\partial r) \quad (5)$$

where by setting $k = 0$, 1 or 2, the equations may be written for cartesian, polar or spherical co-ordinates, respectively.

Provided the detailed kinetics of the reaction processes are known, or some simple relationship between both the overall reaction rate and the diffusion coefficients and the gas properties of pressure and temperature may be assumed, a solution is possible (Sp57). The method allows, e.g., the time-history of the development of a steady-state flame to be computed (Bl73).

Vance and Krier (VK74) have presented a model for spherical and cylindrical flames using a modified form of the above relationships which attempts to predict the behavior of flames in the presence of conductive and convective heat loss. They report a fair degree of success with their method.

As is evident from the foregoing discussion, a comprehensive solution to the problem of burning velocity and flame structure calculations requires a detailed knowledge of the reaction mechanism for laminar flames. Even then, the success of the analytical approach may only be assessed by comparison with reliable experimental data. In most instances, such data is only available over a limited range of pressures and temperatures, albeit usually for the full range of mixtures between the flammability limits. At the present time, confusion still exists with the burning velocity data of most fuels as "conflicting results continue to be published" (AB72). Most authors who currently approach the problem from the experimental point of view attempt a correlation with the analytical results based on some simplified reaction scheme (BH71) with limited success.

These two methods of studying flame propagation—analytical and experimental—are clearly complimentary and interdependent. The analytical approach requires reliable experimental data both for its execution and for comparison to assess its success. On the other hand, the achievement of good experimental values relies on some of the results of the theoretical studies for its accuracy. In this context, the corrections to burning velocity for flame thickness, reported in Section 7.2, depend materially on the temperature profiles through flames at pressures where it is most difficult to measure them, due to the small thickness of the flame front. Analytical models can provide valuable information in the determination of such correction factors.

4. LAMINAR BURNING VELOCITY

One of the most important intrinsic properties of any combustible mixture is its laminar burning velocity and the dependence of this property on such variables as mixture composition, temperature and pressure. Hopefully, as has been suggested in the previous section, this observable macroscopic effect will ultimately yield to analytical studies—as may such altogether more complex phenomena as turbulent flame velocity and knock in spark-ignition engines. In the meantime, however, there is a wealth of experimental evidence to suggest that laminar burning velocity is an important variable in correlation equations for such phenomena as flashback and flame-tilt in burners, minimum ignition energies of electric sparks, and turbulent flame velocity—to mention but a few (LV61). Evidently, therefore, an accurate knowledge of this property, together with the influence of other variables on it, is important in any combustion study.

The ignition of a combustible homogeneous mixture from some point within it results in the propagation of a flame. The velocity of spread of such a flame relative to the point of ignition is readily measurable. However, this *spatial velocity* (S_s) is not a unique property of such a mixture. It can be shown to be the sum of two velocities, namely the *burning* or *transformation velocity* (S_t) and the *unburnt gas velocity* immediately adjacent to the flame front (S_{ug}): i.e.

$$S_s = S_t + S_{ug}. \tag{6}$$

The second and generally larger component (S_{ug}) is apparently a function of the relative densities of the burnt and unburnt gas at any instant, as well as of the presence or absence of any constraining boundary.

The burning velocity (S_t) is defined as the relative velocity, normal to the flame front, with which the unburnt gas moves into this front and is transformed. It is considered to be an intrinsic property of the specific combustible mixture. Symbolically, it can be expressed as (RP62)

$$\begin{aligned} S_t &= -(1/A_f \rho_u)(\mathrm{d}m_u/\mathrm{d}t) \\ &= (1/A_f \rho_u)(\mathrm{d}m_b/\mathrm{d}t) \end{aligned} \tag{7}$$

where A_f is the flame front area, ρ_u is the unburnt gas density immediately adjacent to this area, and $(\mathrm{d}m_u/\mathrm{d}t)$ is the mass rate of flow of unburnt gas into the flame front, which is equal to the mass rate of formation of burnt products $(\mathrm{d}m_b/\mathrm{d}t)$.

The methods used for determining laminar velocity fall into two categories: those in which the flame front remains stationary in space, i.e. $S_s = 0$ or $S_t = -S_{ug}$, and those in which it moves with respect to some fixed point—usually the point of ignition.

The first category can be subdivided into two classes: namely, diffusion flames and premixed flames. Examples of the former are the burning of candles, oil wicks, wood or coal. The best example of a premixed flame is that obtained in a Bunsen burner. When the combustible gases are premixed and the flow is laminar this yields the characteristic inner cone and mantle of all burner flames.

Propagating flames may also conveniently be subdivided into two classes: namely constant volume and constant pressure. Examples here are the spherical constant volume vessel, soap bubble and cylindrical tube methods. Their study requires a means of measuring the velocity of propagation of the flame-front relative to the fixed point of ignition (S_s), as well as a means of determining the unburnt gas velocity (S_{ug}).

The former may be achieved either photographically using direct, Schlieren, shadow or interferometric methods; or by the use of ionization gaps, fusing wires, temperature probes or similar devices capable of detecting the flame front. The latter (S_{ug}) may either be determined analytically or by using some velocity measuring device, such as a hot-wire anemometer. If suitable particle tracking techniques for observing the gas motion in both the unburnt and burnt regions can be developed, then S_t follows directly from eq. (6). In the constant volume method an additional desirable observation—if full advantage is to be taken of this method—is the change in pressure in the vessel during the course of the flame.

Each of the foregoing methods has certain advantages and disadvantages. These will be discussed in greater detail in Section 6.

5. FUNDAMENTAL PROBLEM IN BURNING VELOCITY MEASUREMENT

Many of the difficulties associated with the determination of laminar burning velocity centre around the precise meanings given to the variables in eq. (7)—and in particular to the flame-front area A_f.

The case of an infinite plane flame, in which the flame front is normal to the direction of flow of the unburnt gas, is the only one in which these difficulties do not arise. In all other systems ". . . no definition free from all possible objections can be formulated" (Li53). Unfortunately, the closest approximation to an infinite plane flame, the flat-flame burner of Powling and Edgerton (Po49, Po61, ET52), is limited in this as well as other respects.

The basic question to which an answer is required is therefore: Which part of the flame should be selected for measurement purposes? Evidently, from eq. (7), any surface within the flame front at which the corresponding values of density (ρ) and mass flow rate ($\mathrm{d}m/\mathrm{d}t$) can be accurately and reproducibly determined would be acceptable. Undoubtedly, the best surface is that at which the temperature just starts to deviate from the unburnt gas value (T_u, Fig. 1). Unfortunately, due to the asymptotic nature of the temperature profile this position is unmeasurable. Temperature or density measuring devices of high spatial resolution and sensitivity, such as Schlieren photography or laser interferometry (Ga76), would seem to be indicated—provided corresponding values of area and temperature are used in eq. (7).

Fristrom has shown that the inner region of the

luminous zone represents the best location at which to measure gas velocities and areas for curved thick flames (Fr65). Using eq. (7) he defines a burning velocity, S_t^*, immediately adjacent to the reaction surface of area A^*, and density, ρ^*, as

$$S_t^* = (A'\rho'/A^*\rho^*)S_t,$$

where A', ρ' and S_t' are the values measured at some other surface.

5.1. *Methods of Observing the Flame Front*

Various methods of locating the position of the flame front have been proposed and used (DS57). These include:

(1) Direct photography of the luminous flame (LP51, GW53, SE59).
(2) Shadow photography using a point source of light (SL48, GL49, AF49, AF50).
(3) Schlieren photography using either a coarse grating illuminated from behind (GW53, Gi57) or an optical system using lenses or mirrors (CL51, PL51, BW53, Di53, BW54, Se61).
(4) Interferometry (OI49, GW53).
(5) Particle track measurements (photographic or laser Doppler) (Sm37, VL43, AF50, FA54, Fr56, Go76, EP76).
(6) Ionization gaps (ES57, SA57, EA58, Gr59, AG61).
(7) Temperature measurements (KW48, Fr53, GL53, GW53, FB54).

Since the intensity of the luminous zone is generally sufficiently high, particularly for hydrocarbon mixtures, direct photography is possible and has frequently been used. However, as was discussed in Section 2, this zone is located some distance behind the initial temperature rise and hence does not represent the start of the interaction between the unburnt gas and the combustion wave. (Figs 1 and 2). In burner flames, the thickness of the preheat region ahead of the luminous front is found to vary from about 1 mm at atmospheric pressure (AF50) to about 10 mm at 1/20 atmosphere (KW48). This surface would therefore appear to be unsuitable for determining burning velocity (for low-pressure burner flames at any rate) unless the corresponding unburnt gas density can also be measured.

Shadow photography has been studied fairly extensively (SL48, Wo49, AF59), and it has been established that the sharp inner shadowgraph edge is dependent on the distance between the flame and the screen or photographic plate. Further, this edge is located ahead of the preheat region and approaches the start of this region as the distance between flame and screen is decreased. This well-defined edge may therefore only be used if suitable corrections can be made. On the other hand, the outer shadowgraph edge, which is coincident with the Schlieren edge, and is not dependent on distance, is not well-defined and is hence difficult to measure. For these and other reasons, shadow photography is considered unreliable, and Gaydon and Wolfhard recommend that it be abandoned (GW53).

Of the optical methods, the best measurements of the start of the preheat zone are afforded by the Schlieren, interferometric and particle track methods. Interferometry, although possessing many attractive features, can be expensive and complicated to use. In any case, it is doubtful whether for this purpose it can provide much additional information as compared with Schlieren or particle track techniques.

Schlieren methods yield a focussed image of the flame, enabling the position of maximum intensity, given approximately by $(-1/T^2)(\mathrm{d}T/\mathrm{d}x)$, to be easily located. In burner flames, this apparently occurs at about 200°C (KW48). It has, however, been pointed out that ". . . because of the optical arrangement for photography the Schlieren in a conical flame may be at much lower temperature, and this displacement will depend on the thickness of the pre-heating zone, and therefore on the burning velocity. The Schlieren may thus serve to locate the position of the first temperature increase which is required for measurement of burning velocity" (GW53, p. 67). Smoke (Br49) and particle track (AF50, GL52, Ge53) measurements in burner flames confirm that the flow lines remain parallel to the burner axis until the Schlieren image is reached. There seems little doubt, therefore, that wherever possible the Schlieren edge should be used for burning-velocity studies (GH50) (Fig. 5).

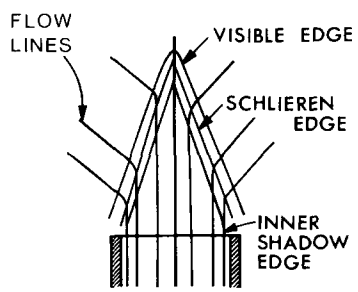

FIG. 5. Relation of flow lines to flame images (GH50).

The particle track method is an extremely versatile technique for the study of flames. By its use, von Elbe and Lewis (VL43) were able to show that burning velocity is a "genuine physical constant" (GW53). However, it is apt to be rather tedious as a means of determining burning velocities *per se*. Care has to be exercised that the particles used do not have any catalytic effects on the flame and also that they are small enough to accurately indicate any changes in direction of the stream tubes. Nevertheless, it is one of the most powerful techniques available (CW63, SG56, AF49, Li76, Li68, RM71, FW65, BS69, EH69).

It has long been known that the electrical conductivity of flame gases is high as compared with the unburnt gas. A method of detecting the position of the flame front as a result of such changes in conductivity (by means of ionization gaps) has been used by Agnew and his coworkers in their studies of flame propagation in spherical constant-volume vessels (Es57, Sa57,

Ea58, Gr59, AG61). Evidently such ionization gaps will trigger at some point within the luminous zone (CK55, KN59). If the flame-front thickness is variable, as it might well be in constant-volume experiments, this technique may introduce significant error. Further, unless care is exercised regarding the probe dimensions, there is a possibility of deforming the flame front due to cooling and/or quenching effects (PB59). Since it appears that the best surface at which to locate the flame front is that at which the temperature just starts to deviate from the unburnt gas value, evidently the most direct determination is via some form of density or temperature measuring device of high spatial resolution and sensitivity.

To summarize, therefore, it would appear that: (1) if an optical method of observing the flame front is to be used then either Schlieren or particle tracking techniques are indicated, and (2) if nonoptical methods are necessary, a density or temperature sensing device of small size, high sensitivity and short response-time would seem to be preferable.

It must be stressed, however, that the bulk of the experimental evidence relating to flame-front structure has been obtained on low-velocity, low-pressure, stationary flames. For such flames, the thickness of the preheat region is given approximately by eq. (2). If this equation is equally applicable to high-velocity, high-pressure propagating flames, the thickness of the preheat zone may not be significant. Any of the above methods would then be equally effective. However, there is a possibility that the controlling mechanisms and reaction schemes deduced from stationary flames may not be applicable to propagating flames (GW53, p. 81). Wherever possible therefore, alternative methods of observing the flame front would appear to be desirable as a check on each other.

6. METHODS OF MEASURING LAMINAR BURNING VELOCITY

Since laminar burning velocity is known to be dependent on the temperature, pressure and composition of the unburnt mixture, any experiment for its determination should ensure accurate control or measurement of these parameters. Further, the flame front should ideally be plane and well removed from any surface which could cause heating, quenching or catalytic effects. If a plane surface is unattainable, then the flame should at least have a large radius of curvature compared with the anticipated flame-front thickness. In such cases, the surface should preferably be one-dimensional, so that it is amenable to rigorous mathematical description, thus permitting reliable corrections for flame-front thickness and curvature to be applied.

On the experimental side, the method should be as economical as possible on fuel, permit wide variations in unburnt gas temperature, pressure and composition, yield reproducible results and, if possible, be simple to use.

The methods which have been used to determine laminar burning velocity have been categorized either in terms of the complexity of their flame-front shapes (Li53, Li54), or in the two classes of stationary and propagating flames (AB72). A combination of these two approaches would seem to be convenient. We will thus treat each of these two classes—stationary and propagating flames—in order of decreasing complexity of their flame-front shapes.

6.1. *Stationary Flames*

Laminar burning velocities can be measured by causing a premixed combustible mixture in which the flow is laminar to enter a stationary flame front ($S_s = 0$) with a velocity equal to the burning velocity ($S_{ug} = -S_l$). Ideally, the flame front should be plane. However, since a stationary flat flame is unstable, some means must be provided for anchoring the flow above the burner mouth. By definition, all such methods distort the flame front to a greater or lesser extent.

6.1.1. *Burner methods*

Burner flames of one kind or another have been studied extensively and have provided valuable insight into a host of combustion problems (Jo46, LV61). As a consequence, most of the earlier burning velocity data available in the literature have been obtained by burner methods (Jo56, GW53, Li53, LV61, AB72). Doubtless, the main reasons for this are that in its rudimentary form the apparatus required is inexpensive, versatile, and superficially easy to use. However, most of the results obtained with such simple apparatus must be considered of doubtful reliability.

Various kinds of burner have been tried—circular tube, shaped nozzle, orifice, and rectangular slot types. In the circular-tube and rectangular-slot types, at appropriately low Reynolds numbers, the unburnt gas velocity profile is parabolic, whilst suitably designed nozzle and orifice burners yield essentially uniform velocity profiles (except in the boundary layer) and straight-sided flame cones (Fig. 6).

In essence, these methods entail establishing laminar flow in a vertical conduit, the flame being held stationary at the top end by the flow of combustible gases. Since the spatial velocity, S_s, is then zero, the burning velocity, S_l, at any particular point on the flame-front cone is numerically equal to the normal component of the gas velocity at that point. That is (Fig. 7)

$$S_l = S_{ug} \sin\alpha. \tag{9}$$

Alternatively, the average burning velocity over the whole flame-front cone can be obtained from mass continuity, thus

$$S_l = \dot{m}/\bar{\rho}_u A_f. \tag{10}$$

A preferable, but more tedious, approach to the foregoing is the use of particle tracking, so successfully demonstrated by Lewis and von Elbe (LV61) and Levy and Weinberg (LW59) (see Fig. 8). In this technique, stroboscopically illuminated particles provide direct

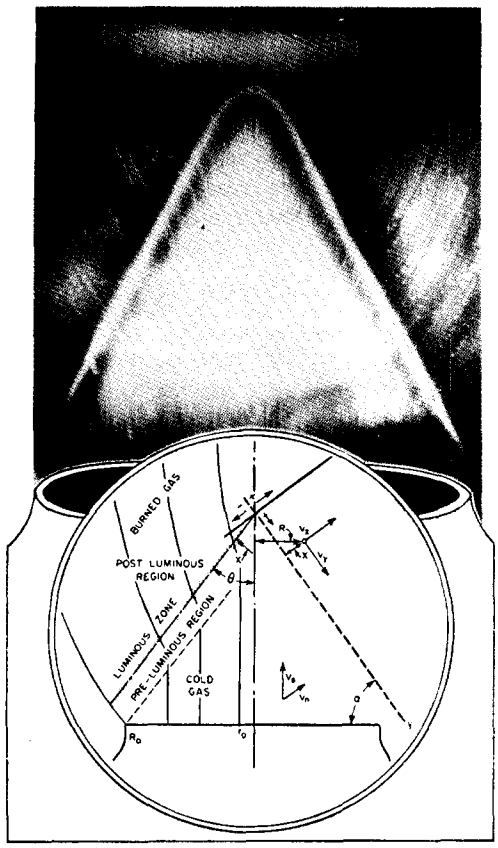

FIG. 6. Nozzle burner with straight-sided flame cone (Fr57).

measurement of both the velocity and direction of the containing streamtube. Use of this method enabled Lewis and von Elbe (LV61) to show that the flame velocity was constant over most of the flame front (Fig. 9). Results using this approach, or modification thereof, are reported in Refs AF49, SG56, CW63, Li67a, Li68, RM71, FW65 and BS69.

One other method which has been used to determine burning velocities in burners is the so-called flame thrust method. From the momentum equation for one-dimensional flow it can be shown that the pressure difference across a flame front is given by (Lv61, GW70)

$$p_u - p_b = \rho_u S_t^2(\rho_u/\rho_b - 1). \tag{11}$$

Measurement of this pressure difference, using a micropitot-tube probe, together with calculation of ρ_u and ρ_b, can yield the burning velocity, S_t. Because of the very low pressure differences available the attainable accuracy is poor. Nevertheless, the approach has been used with some success, particularly for high burning-velocity mixtures (EH69, FW65, BS57, GW60, EH70). Although small, it is this effect which causes divergence of the unburnt gas flow-lines in tube burners and contributes to the rounding of the flame-cone tip (FW65). This divergence is quite prominent in inverted flame cone burners (Fig. 10) which, incidentally, appear to have a number of attractive features when used with particle tracking for laminar burning velocity measurements.

Although essentially simple, burner methods suffer from the following inherent disadvantages:

(1) Lack of uniformity of the burning velocity over the flame surface, particularly at the flame tip and near the burner rim (LV61, GW70).
(2) Difficulty of establishing the relevant unburnt gas temperature profile through any section of the flame cone. Since burning velocities are strongly dependent on unburnt gas temperature, this is an essential piece of information (GR78).
(3) Nonadiabatic nature of the flame particularly near the base of the cone (GW70).
(4) Air entrainment into the flame-cone base, especially with rich mixtures (KU62).
(5) Distortion of the flame cone due to flame thrust (Fr57).
(6) Effects of variable flame-front thickness (GW70).
(7) Catalytic and inertial effects of solid particles when the particle tracking method is used (AF49).

If the use of a burner method is inevitable, then a nozzle or inverted cone burner with particle tracking and Schlieren photography is recommended—particularly if the Schlieren cone can be associated with a particular unburnt gas temperature (KW48, AB72).

Comprehensive reviews of burner methods are to be found in Refs Jo46, LV61, GW70 and AB72.

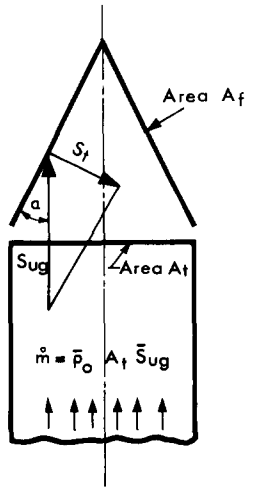

FIG. 7. Flame cone geometry.

6.1.2. *Flat-flame method*

This method, due to Powling and Edgerton (Po61), provides a close approximation to the ideal one-dimensional flat flame, but is unfortunately limited to low burning velocities (0.15—0.20 m/sec). The apparatus used is shown in Fig. 11. Here, the pre-mixed combustible gases enter a cylindrical burner tube *A*, of approximately 60 mm diameter, from below. After being evenly distributed across the whole diameter of the tube by a matrix *E*, glass bead packing *B*, and fine diffusion screens *C*, the mixture enters the vertical channels of the matrix *D*. This matrix is built up of alternate layers of plain and corrugated metal tape, as

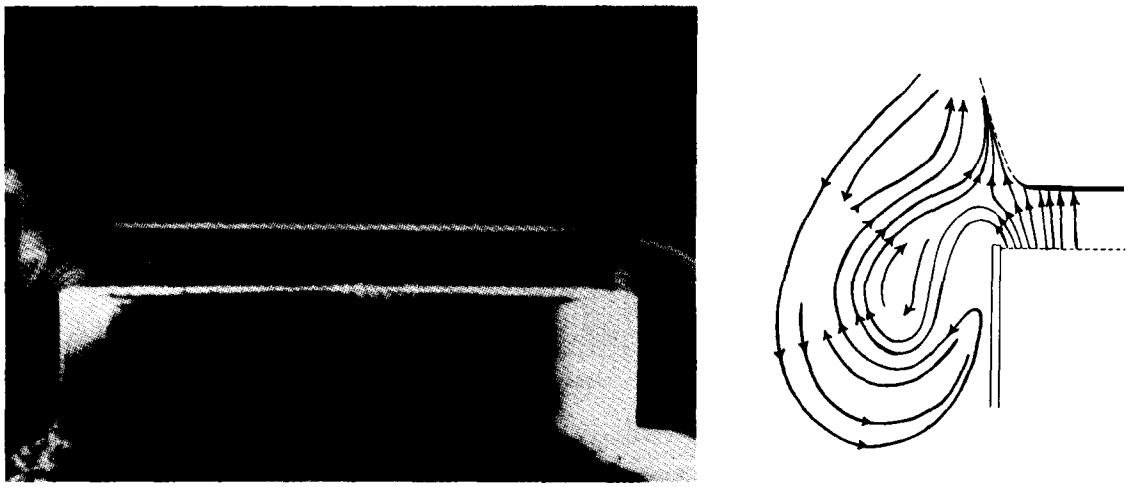

FIG. 8. Particle track photograph of a flat flame with sketch of direction of observed flow (LW59).

shown, resulting in a unit of high density and low pressure drop. In passing through the channels of D, any turbulence in the gas is eliminated and laminar flow is set up in each channel. The distance of the top of D below the burner port is adjusted to a value (usually 5–10 mm) such that these irregularities in velocity are eliminated, but parabolic flow has not begun to be established in the main burner tube. A wire gauze or perforated asbestos board placed above the flame serves to stabilize it by setting up a system of vortices on the flame rim (Fig. 8) (LW59). The resulting flame has the appearance of a flat disk with a slightly curled-up edge. The area of this disk divided into the volumetric flow-rate of the mixture yields the burning velocity.

Since flow rates can generally be accurately determined the accuracy of this manner of using the method would appear to depend on the measurement of the disk diameter. However, the particle track photographs of Levy and Weinberg (Fig. 8) (LW59) suggest that some unburnt gas may escape at the flame edges, thus lowering the calculated value of S_t. Also, because of mixing and cooling by the surrounding nitrogen, the exact position of the flame edge is uncertain. It is claimed that provided the burner diameter is large, the error from this cause is small. But for flame stability reasons, large diameters may only be used for slow burning mixtures. Faster flames require narrower burners. Alternatively, concentric nozzle burners may be used. Powling (Po61) claims that with such an arrangement, essentially flat flames can be obtained up to burning velocities of about 1.0 m/sec.

Another disadvantage of this method is the heat loss from the flame and associated heating of the matrix. The former renders the flame nonadiabatic, the latter peheats the unburnt mixture—lowering and raising S_t, respectively. Botha and Spalding (BS54) used a porous sintered bronze plate for stabilizing the flow, and measured the heat transferred to this plate at various flow rates. By extrapolating the ratio of the volumetric flow rate to flame disk area ("apparent burning velocity") to zero heat transfer, it is claimed that true adiabatic burning velocities were obtained. This seems a reasonable claim, particularly since the unburnt gas temperature, T_u, would be controlled by the water cooling provided.

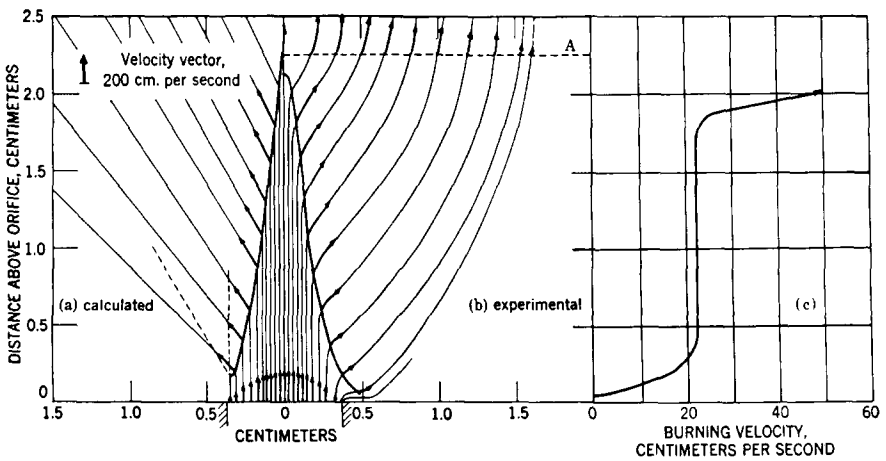

FIG. 9. Combustion-zone flame pattern and burning velocity determined through vertical centre plane of a natural gas–air flame on a rectangular burner tube (LV61).

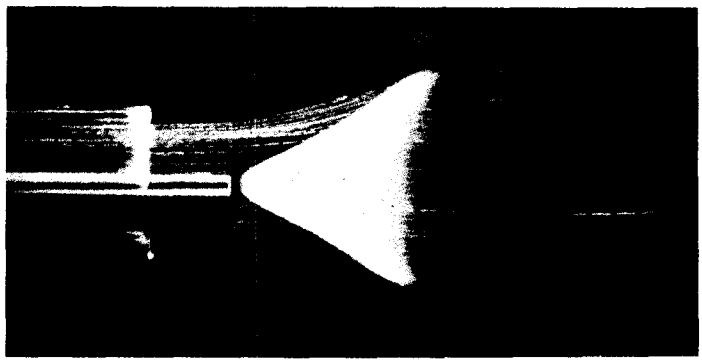

FIG. 10. Inverted flame-cone with particle tracks (LV61

Because of the foregoing difficulties, Levy and Weinberg (LW59) prefer the use of particle tracking techniques with flat-flame burners. Dixon-Lewis and Williams (DW67) using this approach have reported higher values for methane–air than those obtained by the area method (ET52). Both Botha and Spalding's results for propane–air (BS54) and Edmondson and Heap's for methane–air (EH70) are lower than those obtained by the particle-track–cone-angle methods using nozzle burners. Some doubt must, however, be expressed about the relevant value of T_u in these latter experiments.

6.2. *Propagating Flames*

The ignition of a quiescent, homogeneous combustible mixture from some point within it results in the propagation of a flame. The subsequent spread of such a flame is determined, *inter alia*, by the nature of the bounding surface between the mixture and its surroundings. Three types of bounding surface have been used: rigid cylindrical tubes, either closed at both ends or open at one or both ends; soap bubble solutions or thin elastic membranes; and, rigid spherical vessels.

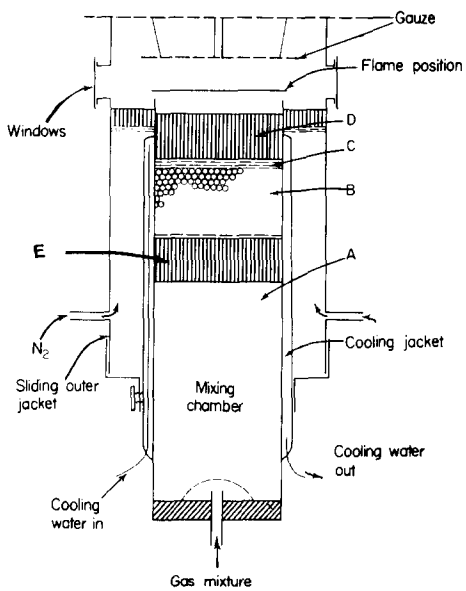

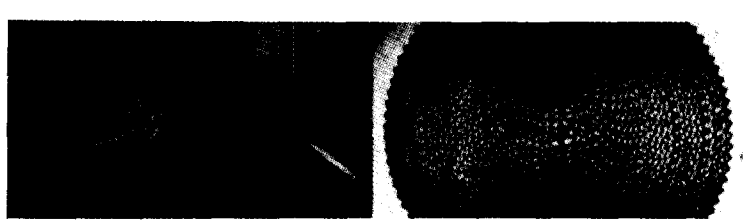

FIG. 11. Flat-flame burner (Po61).

6.2.1. *Cylindrical tube methods*

The early literature contains many values of flame speeds measured in tubes (BT27, Jo46, LV61). However, it is doubtful whether these results are of any significance in determining burning velocity, since this method is subject to serious wall interaction effects, one result of which is to deform the flame front. Thus, the spatial velocity of any given mixture may increase many times—as a result of less wall interaction—as the tube diameter is increased (Fi43). However, vibrations usually then set in, and the flame-front shape tends to become irregular and difficult to measure. Also, different values are obtained depending on whether the flame propagates in an upward, downward or horizontal direction. Certainly, other than for tube diameters close to the quenching distance, flame-front vibrations appear difficult to avoid, particularly for mixtures ignited by means of a spark rather than an open flame. The excellent set of photographs given by Fiock (Fi43) illustrate some of these points (Fig. 12).

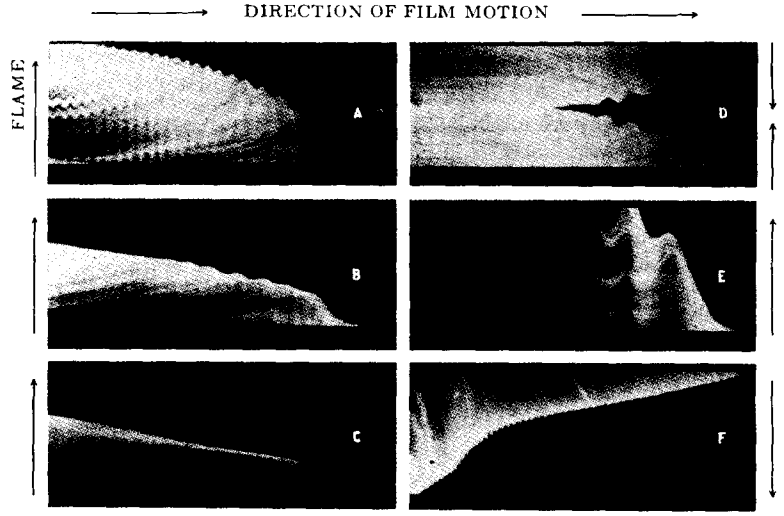

FIG. 12. Typical records of explosions in closed and open-ended tubes (Fi43). A, B, C—tube closed at both ends, initial pressure 1, 2/3, and 1/3 atmosphere respectively. D—tube closed at both ends, initial pressure 1 atmosphere, fired simultaneously at both ends. E—top end of tube open, pressure 1 atmosphere, fired at closed end. F—top end of tube open, pressure 1 atmosphere, fired at open end.

In essence, the method as used by Coward and Hartwell (CH32, CP37) consists of a long cylindrical tube closed at one end and filled with the gas mixture under test. Ignition at the open end results in an initially uniform flame travelling towards the closed end (F in Fig. 12). Measurement of this uniform velocity, S_s, together with the area, A_f, of the pseudo-hemispherical flame-front yields an average burning velocity via the following equation, directly derivable from the defining eq. (7):

$$S_t = S_s \pi R^2 / A_f \tag{12}$$

where R is the tube radius.

The provision of a small hole at the end of the tube towards which the flame travels, and a larger one at the other end, apparently renders the flame movement uniform, stable and reproducible (GM48, GL51). Most subsequent workers have used this revised tube method (Co61, GL51, CL59, HH56, EP69). The relevant equation now becomes (GM48)

$$S_t = (S_s - S_{ug}) \pi R^2 / A_f. \tag{13}$$

Here the unburnt gas velocity, S_{ug}, is determined from the displacement of a soap bubble formed over the orifice at the unburnt-gas end.

In a further adaptation of this method, Fuller *et al.* (FP69) ignited the mixture at both ends, thus producing a double-flame kernel with relatively flat flame-fronts—thus reducing the error in determining A_f. This is similar to the technique used by Raezer and Olsen in a spherical vessel (RO62) (see also Fig. 12D). Provided vibrations can be avoided and the unburnt gas between the flame kernels is stationary, then $S_t = S_s$. However, T_u and p_u also need to be measured if they do not remain constant.

Even with all the above refinements, it is doubtful whether the wall interaction effects can ever be adequately corrected for. On the whole, therefore, the method appears to be inherently unsatisfactory.

6.2.2. *Flame kernel method*

Following on theoretical and experimental work by Dery (De49) on the ignition, growth and transport of a flame kernel in a laminar combustible gas-stream, Bolz and Burlage (BB55, BB60) attempted to use this technique to measure burning velocity. Measurements of the flame area and hence the radius of an equivalent sphere as the flame kernel was carried downstream, yielded S_s, from which S_t was determined from the equation

$$S_t = (\rho_b / \rho_o) S_s = \alpha S_s \tag{16}$$

the density ratio, α, being determined from thermochemical calculation. The method has the advantage of removing the flame from the influence of the spark electrodes, but suffers from the disadvantage of a complex flame-front shape since the kernel is not spherical.

In an adaptation of this approach, Raezer and Olsen (RO62) produced two flame kernels by simultaneously igniting a combustible mixture at two separate points in a combustion vessel. Since the unburnt gas velocity on the axis joining the two ignition points must be zero as the kernels propagate towards each other, then, from eq. (6), $S_t = S_s$. In theory, provided that ignition is simultaneous, the pressure rise is small, and the gas between the kernels is quiescent, this method should yield reliable results.

A recent modification by Andrews and Bradley (AB73) of this method appears to have yielded good results. Two flame kernels propagate towards one another such that their flame speeds as they meet tend towards the burning velocity. The kernels are contained in a cylindrical vessel with double ignition, and measurements are taken during the constant pressure period of combustion. Spark synchronization problems generally resulted in kernels of different sizes. Satisfactory results are claimed when the size discrepancy is not too large. The method is apparently beset with considerable experimental difficulty, resulting in a low success rate with firings. An advantage of this technique is that flame curvature and thickness corrections are not required.

A possible adaptation of this approach might be to use two partially intersecting soap bubbles or latex balloons, which are simultaneously ignited.

6.2.3. *Soap-bubble method*

Of the techniques which are essentially independent of solid surfaces, possibly the simplest is the soap-bubble or constant-pressure method devised by Stevens (St23), and developed by Fiock and Roeder (FR35) and Linnett *et al.* (LP51). Here the combustible mixture to be tested is used to blow a spherical bubble around a central spark gap. Provided such a bubble offers no significant resistance to gas expansion, ignition of the mixture results in the propagation of a spherical combustion wave at essentially constant pressure. (For relatively low velocity flames, the pressure field across the flame front may generally be ignored. Significant error may be introduced in high velocity flames if the pressure is assumed constant.) For purposes of analysis, the bubble is photographed through a narrow horizontal slit using a drum camera. A typical record is shown in Fig. 13, from which it is seen that the spatial velocity, S_s, is essentially constant throughout the process.

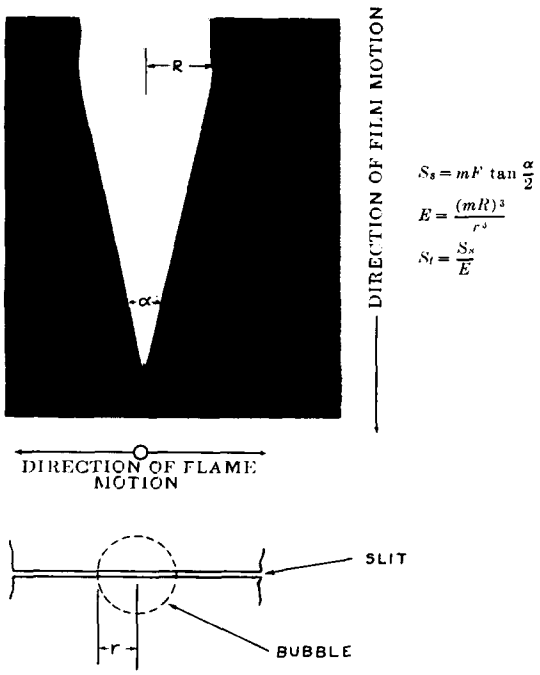

FIG. 13. Typical record of an explosion in a soap bubble (Fi43).

Now, for a spherical flame front of negligible thickness

$$A_f = 4\pi r_b^2$$

whilst the mass of burnt gas, of constant density ρ_b, is

$$m_b = 4\pi r_b^3 \rho_b/3.$$

Hence,

$$dm_b/dt = 4\pi r_b^2 \rho_b (dr_b/dt).$$

Also,

$$\rho_u = \text{constant} = \rho_o.$$

Hence, from our definition of burning velocity (eq. (7)),

$$S_t = (\rho_b/\rho_o)(dr_b/dt) = \alpha S_s. \tag{15}$$

Thus, provided the density ratio, α, can be measured or calculated, and S_s determined from the photographic trace, then S_t follows. Generally, α is obtained from measurements of the initial diameter of the spherical bubble, $2r_o$, and the final diameter of the burnt gas, $2r_e$, since for conservation of mass

$$\alpha = (r_o/r_e)^3. \tag{16}$$

The accuracy of the method is thus evidently very sensitive to errors in r_o and r_e. Although it is generally possible to measure both S_s and r_o accurately, the determination of r_e can present difficulties. As a result of afterburning it may not be possible to establish a precise value for the final diameter (Li53, SS53). Inertial effects should also become significant at higher velocities (Si59, SW53). Surface irregularities certainly then become apparent. Also, for low-velocity flames, buoyancy introduces distortion of the burning sphere.

An alternative method of determining α is via thermodynamic calculations (Ga73). Close agreement with observed values has been reported (SW53, SE59). It is suggested that wherever possible both methods be used.

A decision as to the use of Schlieren or direct photography for observing the flame front does not arise here, since, because of the constancy of S_s, both techniques should yield the same results (LP51, PL51). Also, since burning velocity equations for thick flame-fronts are now available (GR75), it is possible to correct for the effects of curvature.

A disadvantage of this method is that if water-based

soap solutions are used, dry mixtures cannot be tested (SW54). However, nonaqueous soap solutions based on glyserol have proved quite successful (SS53, SE59). Also, it has been suggested that diffusion of the mixture through the bubble wall may be sufficiently great to alter its composition (LV51). No evidence of this has been found with either acetylene–air mixtures (LP51) or with ethylene–oxygen–helium mixtures (ML53). In any event, the use of transparent latex rubber balloons should obviate this difficulty (PP53, SE59).

Two important advantages of this method are its use of only small quantities of combustible mixtures and the ability provided to vary both initial temperature (within narrow limits) and pressure (within wide limits). In terms of the burning velocity range, low velocities lead to buoyancy and heat-loss effects, whilst high velocities (25 m/sec) produce surface irregularities (Si59). At intermediate velocities, this method yields good results (LP51).

6.2.4. *Spherical constant-volume vessel method*

The so-called spherical bomb method has not been used as extensively as many of the others, although it has been described by Linnett as ". . . potentially a powerful method for determining burning velocities" (Li53). If its full potentialities are used it can yield considerably more information from a single experiment than can any other method. Also, to quote Lewis, ". . . the method is self-corroborating, and since the experimental precision is very high, it must be regarded as a precision method and, at the same time, a standard method against which the validity of other methods can be tested" (Le54). Its limited use to date has perhaps been due to a lack of understanding of the underlying theory, coupled with some doubts about the possible errors introduced during the early stages of combustion by the influence of the spark, of flame curvature, and of flame-front thickness, as well as its relative analytical and experimental complexity. Hopefully, most of this uncertainty has been eliminated over the years as these problems have been progressively overcome or shown to be unimportant (OR59, RP62, RT63, Ra63, RG65, RG65a, RG65b, Ga73, Ga74, GR75, GR75a, GR76, GR78).

In this method, a premixed combustible mixture contained in a thick-walled spherical vessel is ignited at the centre. Provided the differences in concentration and diffusivity between the various constituents are not too large and the spatial velocity is not too low, the resulting combustion wave is generally isotropic. The propagation of the flame towards the wall of the vessel is attended by a pressure rise which results in a temperature increase of the unburnt gas. When these changes in pressure and temperature, as well as the position of the flame front, are accurately measured, the method becomes extremely versatile. The effects of both pressure and temperature on burning velocity can then be obtained, over a fairly wide range, from a single experiment. A limited set of experiments can thus provide three-dimensional S_l–p–T surfaces for mixtures of given equivalence ratio (ϕ) (RG65, GR78). Alternatively, any three of these four parameters can be represented on such a map.

Although Hopkinson (Ho06) used combustion in a constant-volume vessel for determining the mean heat capacities of gases at high temperatures, Nagel (Na07), and Flamm and Mache (FM17) appear to have been the first to derive equations relating the pressure at any instant to the volume of gas burnt (LV51, Jo46). Later, Ellis and Wheeler (EW27, El28), with their classical photographs of combustion in a glass sphere, showed that, provided the spatial velocity was not too low, the flame propagates isotropically. However, the initial development of the spherical constant-volume vessel technique for determining laminar burning velocities appears to have been due to Lewis and von Elbe, and Fiock and his associates (LV34, LV61, FK35, FM37, FM40). Using a simplified form of the Flamm and Mache equation, Lewis and von Elbe derived an approximate expression for the mass-fraction burnt, in terms of pressures, which is valid during the early stages of combustion when the pressure rise is small. This enabled them to determine burning velocities during this period. As a check on their assumptions, they compared calculated and observed values of flame-front radius and found very good agreement (MV53). At about the same time, Fiock *et al.*, in some excellent papers, reported on their analytical and experimental work using this method (FK35, FM37, FM40). Unfortunately, both these groups used either restricted or unsatisfactory forms of burning velocity equations.

In 1953, Manton *et al.* (MV53) used an equation attributed to Dery, in which only the time derivative of the flame radius was required. Results on stoichiometric propane–air showed good agreement (for mass-fractions burnt of less than 0.01) with equations involving both pressure and radius. Agnew and coworkers (SA57, Es57, EA58) proposed and used several equations, which included an allowance for the finite velocity of propagation of pressure waves—necessary for very high velocity flames. Unfortunately, these are only applicable to the early stages of combustion. Grumer *et al.* (GC59) produced a modified form of equation for mass-fraction burnt, for which they claim greater accuracy than that proposed by Lewis and von Elbe. O'Donovan and Rallis derived an equation for mass-fraction burnt which is valid throughout the combustion process. Subsequent to this, Rallis and coworkers derived a complete set of equations, as well as a variety of corroborative relations, and showed that all previous equations were particular cases of this general set (RT63, Ra63, Ra64). They used a particularly stable form of equation—referred to as the combined equation—to determine the effects of equivalence ratio, pressure, and temperature on the burning velocity of acetylene–air mixtures, and showed that the nature of the pressure and temperature dependence appeared to be more complex than had hitherto been supposed (RG65).

At this period in time, concern still existed regarding the use of certain assumptions in the theory of this method, as well as with the computational complexity associated with its correct use. Specifically, these were that (GR78):

(1) the flame front remains smooth, spherical and centered on the point of ignition;
(2) the pressure at any instant is uniform throughout the vessel—i.e. there are no pressure gradients or time lag effects in the measurement of pressure;
(3) both the burnt- and unburnt-gas regions are adiabatic systems—i.e. there is no heat loss or gain from these regions;
(4) the effects of flame-front thickness and curvature are negligible;
(5) the burnt-gas density immediately behind the flame front, ρ_f, is an accurate approximation to the instantaneous spatially-averaged density of the burnt gas, $\bar{\rho}_b$;
(6) chemical equilibrium is achieved immediately behind the flame front—i.e. the temperature at this point corresponds to the theoretical equilibrium adiabatic value;
(7) no dissociation or preflame reactions occur in the unburnt gas region;
(8) the required methods of calculating gas properties are complex and tedious.

We will now deal with each of these in turn.

6.2.4.1. *Flame-front irregularities.* For low burning velocity mixtures, the effects of buoyancy, especially in large vessels, can introduce errors. A check on this is provided by photographing the flame through a vertical slit and measuring the flame radii both above and below the spark. Care has to be taken to correct for any slit-width effects (Ra63). Where any discrepancies are found, approximate corrections for the flame propagating as an oblate or prolate spheroid can be applied (Ra63). In any event, checks can be made between the observed and calculated radii (MV53, Ra63). Flame-front irregularities at high velocities and pressures, as observed in constant-pressure experiments by Strauss and Edse (SE59) and Simon and Wong (SW54), are a possibility. These may be caused by acoustic waves set up by the flame and reflected by the walls. No evidence of such oscillation has been observed to date, even with acetylene–air mixtures (Ra63, RG65, Ga75). This is no guarantee that they may not occur at higher velocities and pressures.

6.2.4.2. *Pressure uniformity.* Various writers have examined the pressure distribution through a flame front (LV61, Es57, EA58, Gr59, Ra63, Ra64). The pressure profile in a spherical constant-volume vessel is variously dependent on ρ_u, ρ_b, S_s and S_t (Ra63, Ra64). At low velocities and densities its effects are insignificant. Agnew and coworkers have developed approximate burning-velocity equations which suggest that corrections become necessary when S_s is greater than one-tenth the velocity of sound in the unburnt gas (Es57, EA58). Rallis has shown that correcting for the time-lag for information to be transmitted from the flame front to a pressure transducer on the wall significantly reduces any discrepancy between the observed and calculated pressures, except close to the bomb wall (Ra63).

Babkin and coworkers have derived an approximate equation for correcting the final pressure, p_e, for heat-loss and quenching effects when the flame is in close proximity to the wall (BK65, BV66). Thus, both from theoretical and experimental points of view (of accurately observing the flame-front radius close to the wall due to internal reflections (GR78)), it would appear undesirable to place undue reliability on results obtained for flame-front radii, r_b, greater than about 90% of the bomb radius, R.

6.2.4.3. *Heat loss.* Transfer of heat may occur during the combustion process by radiation from the burnt gas to the unburnt gas and to the containing wall; by radiation and conduction from the unburnt gas to the wall; and by conduction along the spark electrodes. Rallis estimated that for acetylene–air mixtures the heat lost by radiation from the flame to the wall and by conduction along the electrodes was negligible (Ra63). Calculations indicate that this is still likely to be the case, even for much lower velocity mixtures. Garforth developed an infinite–fringe laser interferometer, with which he measured the density close to the wall of the unburnt gas during combustion of methane–air mixtures (Ga74, Ga75). He showed that for a stoichiometric mixture, the calculated adiabatic temperature and that determined from measurements of density and pressure never deviated by more than 1% at the early stages of combustion and $2\frac{1}{2}$% at the end. For slower-burning mixtures this difference may be larger. There is a remote possibility that this small difference may be the result of an equilibrium situation prevailing between heat loss and gain by the end gas. The corroborative relations used in this method (Ra63, GR78) suggest that this is unlikely, but an unambiguous answer will have to await continuous measurements of the flame front temperature, T_f (see sub-Section 6.2.4.6).

6.2.4.4. *Flame-front thickness and curvature* would appear to go hand in hand, since the effect of the latter is negligible when the flame front is considered "thin". As mentioned in the introduction to Section 5, any surface within the flame front, at which corresponding values of area and density are measured, can in principle be used as a reference to specify buring velocities. However, with "thick" flames in a spherical bomb, the mass of gas contained in the flame front, particularly at the early stages of combustion, can account for a significant proportion of the mass of burning and burnt gas. If the more stable burnt gas or combined forms of equation are used (RG65), the assumption that this mass has all burnt can introduce an appreciable error (AB72, GR78) (see also DS74).

Babkin *et al.* (BK62) derived an approximate re-

lationship for the burning velocity of a spherical gas-pocket with inward flame propagation, in terms of the plane-flame value and the flame-front thickness, and showed that flame-curvature effects are significant for $r_f < 3$ mm. Andrews and Bradley (AB72a) did an approximate analysis of constant-pressure spherical-flame propagation with central ignition, including the mass of gas contained in the flame front, and showed that at a flame radius of 25 mm with $p = 1$ atmosphere, $T_u = 300$ K and a flame-front thickness of 1.1 mm, the thin-flame equations were probably in error by as much as 22%. Garforth and Rallis derived a more rigorous set of "thick flame" equations (GR75), with the aid of which they showed that the corrections for methane–air mixtures are not as large as suggested by Andrews and Bradley (GR78). In any event, it is during the early stages of combustion, when the pressure is essentially constant, that the results are most uncertain. Yet this is the region most favored by previous investigators for determining burning velocities. Although the results reported on stoichiometric methane–air mixtures (GR78) must be regarded as tentative (in that the corrections for flame-front thickness are based on an equation derived from results on low-pressure burner flames (DW51)), it is confidently expected that these values of burning velocity are not likely to be more than 5% low in the range $1.1 \leq (p/p_o) \leq 6.0$, nor more than 9% in error outside this range (Ga75, Ga77).

6.2.4.5. *Average burnt-gas density.* Lewis and von Elbe recognized that due to recompression and gas movement there would exist a temperature, and hence density, distribution in the burnt gas (LV61). Using an approximate expression for the mass-fraction burnt (but ignoring gas movement) they calculated this distribution for hydrogen–oxygen and ozone–oxygen combustion in a spherical vessel. Rallis *et al.* (Ra59, Tr62, Ra63) provided a simple expression for calculating the average burnt-gas density, assuming the distribution of density with radius was known, but, because of the lack of an accurate method of analyzing the latter, did not apply it. They instead assessed the error in burning velocity due to the use of ρ_f in place of $\bar{\rho}_b$. The development by Garforth of a computer programme for determining adiabatic equilibrium flame temperatures was the first step in resolving this problem (Ga73). This was followed by an analysis of the gas movement during flame propagation, which thus permitted determination of the distribution of gas properties behind the flame front (GR75a). Fortuitous validation of this analysis was provided by some particle tracks accidentally obtained during certain tests (GR75a, Ga75). The net effect of the correction for both the temperature distribution and gas movement on the values for burning velocity is of the order of 12% (GR78).

6.2.4.6. *Chemical equilibrium.* There is some evidence to suggest that chemical equilibrium is not completely achieved in the flame front (RT63, Ra63). Firstly, there is always an afterglow or reillumination of the burnt gas, which starts from the centre of the vessel before the flame front reaches the wall, and rapidly spreads outwards to reach the flame front at about the same time that the latter reaches the wall (Fig. 14). This strong luminescence persists for some considerable time after the end of the process, gradually collapsing towards the centre as the system cools down (Ra63, RG65, Ga75). The reason for this reillumination has never been explained to our satisfaction, although Lewis and von Elbe consider that it may be due to temperature gradients that exist in the burnt gas with constant-volume combustion, since the same effect is not observed in constant-pressure or open vessel experiments (LV61). Secondly, in all our experiments to date, we have observed that the maximum pressure always occurs a short time after the flame has reached the wall of the vessel (Ra63, Ga75). When incorporated into the expression for $\bar{\alpha}_e = \bar{\rho}_e/\rho_o$, the density ratio at the end of the process, this leads to values which are always less than the value unity, which is theoretically required (RT63, Ga75). Furthermore, the value of $\bar{\alpha}_e$ appears to correlate in the correct manner with spatial velocity and equivalence ratio for acetylene–air mixtures (RT63). The current anticipated error of some 5% in our methane–air results is probably mainly due to this effect (GR78). The question of chemical equilibrium will have to remain unresolved until an adequate means of measuring transient burnt-gas temperature is devised. Possibly the use of a fast-response infrared-radiation pyrometer such as that reported by Penzias *et al.* (PD66) and Shimuzu (Sh73), or a fast-response sodium D-line reversal method might prove successful.

6.2.4.7. *Dissociation or preflame reactions in the unburnt gas regions* do not appear to be significant at the unburnt gas temperatures, and for the range of spatial velocities for which the bomb method has been used to date. The use of an external heater to raise the initial unburnt gas temperature of the mixture, thereby increasing the range of burning velocity values—as suggested by Rallis (Ra63) and used by Babkin and Kazachenko (BK66)—could introduce problems in this regard.

6.2.4.8. *Computational complexity.* That the computational tedium associated with the correct use of the constant-volume bomb is large cannot be gainsaid. However, the use of certain simplifications arising out of the corroborative nature of the method can materially reduce this computational effort without significantly affecting its accuracy (Ra63, Ga75, GR78). As will be shown in the next section, because of the nature of the system, a number of corroborative equations can be derived—usually in terms of the properties of the unburnt and burnt (or burnt and burning) gas, respectively. Strictly, such alternative forms should yield the same results when applied to any given set of experimental data. However, because of the differing sensitivities of the equations to systematic and other

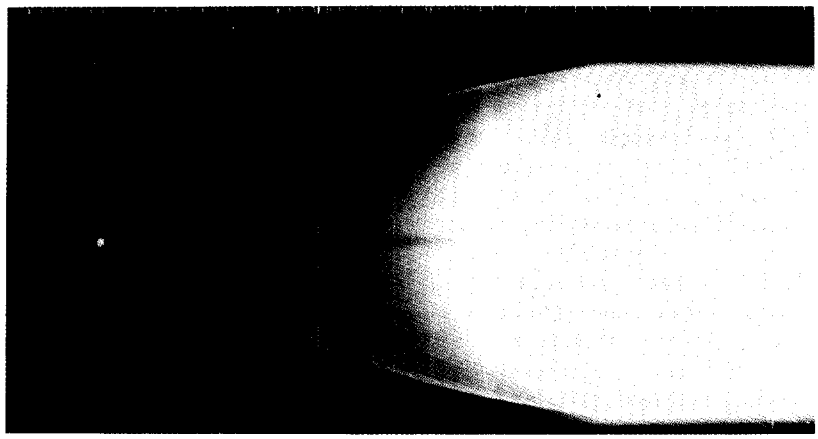

(a) Flame Trace

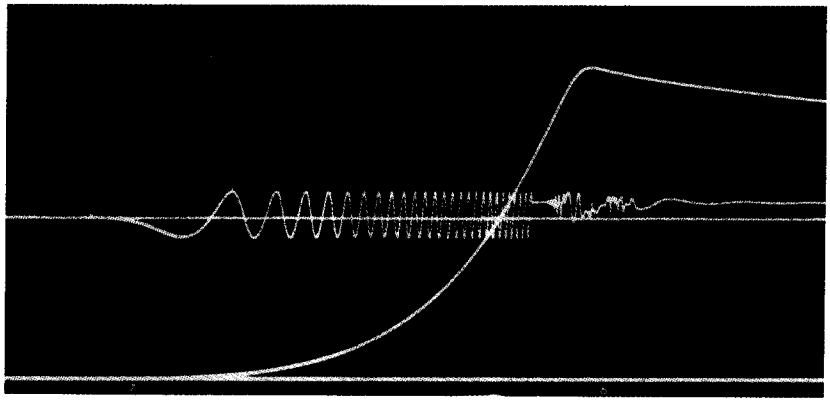

(b) Pressure and interferometer traces

FIG. 14. Typical test records in a spherical constant volume vessel. (a) Flame trace. (b) Pressure and interferometer traces.

errors inherent in the observations, they can lead to slightly different results over the range of the combustion process. This is used to advantage, both for providing indications of the probable source and extent of such errors, and for simplifying the analysis (Ra63, Ga75, GR78).

Consider the burnt-gas density ratio

$$\bar{\alpha} = \bar{\rho}_b/\rho_o. \tag{17}$$

Since the average density of the entire system remains constant throughout the process, and in particular at the end of the process $\bar{\rho}_e = \rho_o$, this can also be expressed as

$$\bar{\alpha} = \bar{\rho}_b/\bar{\rho}_e \tag{18}$$

which must evidently yield the correct end value $\bar{\alpha}_e = 1$. Comparison of the values of $\bar{\alpha}$ from these two equations thus gives an indication of the magnitude of any errors made in calculating $\bar{\rho}_b$.

Figure 15 shows the variations of $\bar{\alpha}$ with pressure ratio (p/p_o), as determined from eqs (17) and (18), calculated for a stoichiometric methane–air test with $p_o = 0.1013$ MPa, (1 atmosphere), including both density-distribution and gas-movement effects. These two curves can be considered as the upper and lower error-bounds in the determination of this important variable. For this test, this error is essentially constant at 4.0% throughout the pressure range. A straight-line fit between α_o from eq. (17) and $\alpha_e = 1$ at $p = p_e$ results in the same value for the maximum apparent error based on $\bar{\alpha}$ from eq. (17). The importance of this lies in the fact that, provided α_o is known or can be calculated, subsequent values of $\bar{\alpha}$ can be obtained from the equation

$$\bar{\alpha} = \alpha_o + (1 - \alpha_o)[(p/p_o) - 1]/[(p_e/p_o) - 1]. \tag{19}$$

It therefore becomes unnecessary for prospective users of this method to enter into the complexity of calculating the flame-front adiabatic temperatures, burnt-gas density distribution, or burnt-gas movement during the process. Equation (19) will yield $\bar{\alpha}$ values well

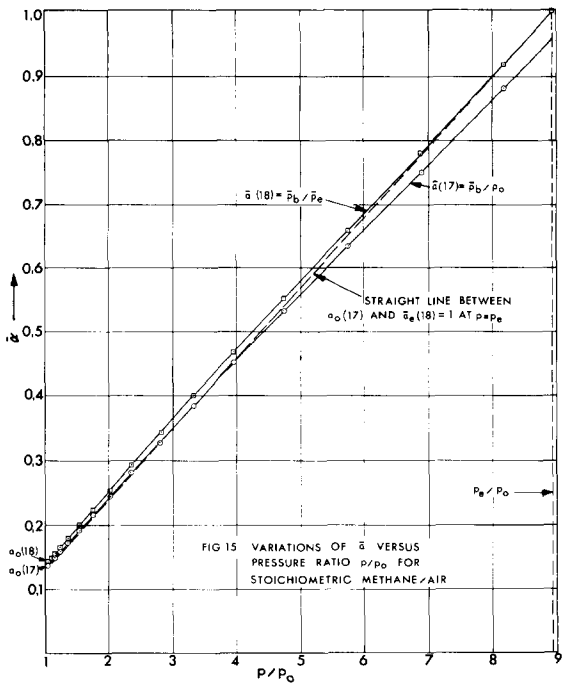

FIG. 15. Variations for $\bar{\alpha}$ versus pressure ratio p/p_o for stoichiometric methane–air.

within the experimental accuracy of the method. However, accurate values of α_o and p are required.

As currently used (GR76, GR78), the constant-volume method has the following important advantages:

(1) Only small quantities of combustible mixture are required.
(2) The mixture composition and initial temperature and pressure can be accurately controlled.
(3) Only a few experiments at different initial pressures, or temperatures, are required in order to establish the separate effects of these parameters on the laminar burning velocity of a particular mixture.
(4) True free-space adiabatic burning velocities can be determined. That is, there are no surface interaction effects and the heat loss is negligible.
(5) Since it has been experimentally confirmed that the variation in mean density ratio $\bar{\alpha}$ throughout the process—allowing both for temperature and density distribution in the burnt gas, and gas movement—is essentially a linear function of instantaneous pressure ratio, the tedium in carrying out the complex calculations required is drastically reduced.
(6) The method is self-corroborative, in that at least two equations or methods of calculating the required variables are available. This permits checks on accuracy—not possible with most other methods. Also, by providing a "carpet" of data, represented by the test curves at different initial pressures with superimposed isobars and isotherms, trends become apparent which assist considerably in proper evaluation of the results (GR78).

Its disadvantages are:

(1) The apparatus required is relatively complex and expensive and the time required to do a test is quite long—of the order of 1 hr for tests in which the initial pressure is not atmospheric.
(2) Transcription of the observations can be tedious unless relatively sophisticated apparatus is available.

7. BURNING VELOCITY EQUATIONS—SPHERICAL CONSTANT-VOLUME VESSEL METHOD

Unfortunately, the majority of users of this method have employed restricted forms of equations which are only applicable to the early stages of the process, when the pressure rise is small. This has seriously restricted its value, virtually relegating it to the status of a constant-pressure technique, albeit with several advantages over the soap-bubble method.

Since we believe this method to be the most precise available to date, a summary of the pertinent equations would seem to be appropriate. These will be presented under two headings: (1) thin-flame equations in which the flame front is considered as a surface of discontinuity and hence infinitely thin, and (2) thick-flame equations for flame fronts having a finite thickness τ.

7.1. *Thin-Flame Equations* (*Ra*63, *Ra*64)

7.1.1. *Basic relations*

For mass conservation

$$m_o = m_u + m_b. \tag{20}$$

Hence, for mass continuity across the flame front,

$$S_t = -(1/A_f\rho_u)(\mathrm{d}m_u/\mathrm{d}t) = (1/A_f\rho_u)(\mathrm{d}m_b/\mathrm{d}t). \tag{7}$$

Defining the mass-fraction burnt as $n = (m_b/m_o)$ yields

$$(\mathrm{d}n/\mathrm{d}t) = (1/m_o)(\mathrm{d}m_b/\mathrm{d}t) = -(1/m_o)(\mathrm{d}m_u/\mathrm{d}t).$$

Hence

$$S_t = (m_o/A_f\rho_u)(\mathrm{d}n/\mathrm{d}t). \tag{21}$$

For isotropic flame propagation in a constant volume spherical vessel:

$$m_o = (4/3)\pi R^3\rho_o \tag{22}$$

$$m_u = (4/3)\pi(R^3 - r_b^3)\bar{\rho}_u \tag{23}$$

$$m_b = (4/3)\pi r_b^3\bar{\rho}_b \tag{24}$$

$$A_f = 4\pi r_b^2 \tag{25}$$

where

$$\bar{\rho}_u = [3/(R^3 - r_b^3)]\int_{r_b}^{R}\rho'_u r^2\,\mathrm{d}r \tag{26}$$

ρ' being some function of r and $r_b \le r < R$, *and*

$$\bar{\rho}_b = (3/r_b^3)\int_0^{r_b}\rho'_b r^2\,\mathrm{d}r \tag{27}$$

ρ'_b being some function of r and $0 \le r \le r_b$.

Evidently, at $r_b = R$, $\bar{\rho}_b = \bar{\rho}_e = \rho_o$.

7.1.2. *Mass-fraction burnt*

Various forms of equation are available for the mass-fraction burnt. Thus, in terms of the properties of the unburnt gas,

$$n_u = 1 - (m_u/m_o) = 1 - \bar{\beta} + \bar{\beta}(r_b/R)^3 \quad (28)$$

whilst in terms of the properties of the burnt gas

$$n_b = (m_b/m_o) = \bar{\alpha}(r_b/R)^3. \quad (29)$$

Also, since strictly $n_b = n_u$, they can be equated to yield a combined form

$$n_t = \bar{\alpha}(\bar{\beta} - 1)/(\bar{\beta} - \bar{\alpha}). \quad (30)$$

7.1.3. *Laminar burning velocity equations*

Differentiating each of the expressions for mass-fraction burnt and substituting into eq. (21) in turn yields three forms of burning velocity equation: i.e. the *unburnt gas equation*—

$$S_u = (\bar{\beta}/\beta)[(\mathrm{d}r_b/\mathrm{d}t) - \{(R^3 - r_b^3)/(3r_b^2\bar{\beta})\}(\mathrm{d}\bar{\beta}/\mathrm{d}t)] \quad (31)$$

the *burnt gas equation*—

$$S_b = (\bar{\alpha}/\beta)[(\mathrm{d}r_b/\mathrm{d}t + (r_b/3\bar{\alpha})(\mathrm{d}\bar{\alpha}/\mathrm{d}t)] \quad (32)$$

and a *combined equation*, a particular form of which is—

$$S_t = \bar{\alpha}(\bar{\beta}/\beta)[(\mathrm{d}r_b/\mathrm{d}t) + \{r_b\bar{\beta}(1 - \bar{\alpha})/3\bar{\alpha}(\bar{\beta} - \bar{\alpha})\}(\mathrm{d}/\mathrm{d}t)(\bar{\alpha}/\bar{\beta})] \quad (33)$$

which contains the spatial velocity $S_s = \mathrm{d}r_b/\mathrm{d}t$ explicitly and is found not to magnify experimental errors.

It should be noted that except for very high burning-velocity flames, the pressure gradient in the unburnt gas is negligible. Thus, for all practical cases, $\bar{\beta} = \beta = (\rho_u/\rho_o)$.

7.1.4. *Corroborative relations*

One of the important characteristics of the constant-volume method is its self-corroborative nature. Thus, it was shown in the foregoing that two basic equations are available for the mass-fraction burnt (eqs 28 and 29) and for the burning velocity (eqs 31 and 32). Other corroborative type equations follows.

Since

$$\bar{\rho}_e = \rho_o = (\bar{M}_e p_e)/(R\bar{T}_e) = (M_o p_o)/(RT_o)$$

the *density ratio*, $\bar{\alpha}$, can be expressed as

$$\bar{\alpha} = (\bar{\rho}_b/\rho_o) = (\bar{\rho}_b/\bar{\rho}_e) \quad (34)$$

and the *maximum pressure* as

$$p_e = (M_o/\bar{M}_e)(\bar{T}_e/T_o)p_o \quad (35)$$

which provides a useful check between the measured maximum pressure and that determined from the calculations of $(\bar{T}_b/\bar{M}_b)$.

Setting eq. (29) equal to eq. (28) and solving for r_b provides an equation for calculating values of *flame-front radius*, which can be compared with the observed values to check on the density ratios $\bar{\alpha}$ and $\bar{\beta}$. Thus

$$r_b = R[(\bar{\beta} - 1)/(\bar{\beta} - \bar{\alpha})]^{1/3}. \quad (36)$$

Finally, if it is assumed that the unburnt gas is compressed adiabatically and that pressure uniformity exists through the vessel, then it can be shown that (Ra63, Ra64)

$$(p/p_e)(r_b/R)^3 + (p/p_o)^{1/\gamma_u}[1 - (r_b/R)^3] \approx 1 \quad (37)$$

from which p can be calculated and compared with the measured values.

The various forms of burning-velocity equations proposed from time to time in the literature can all be shown to be special cases of the foregoing.

7.2. *Thick-Flame Equations (GR75, GR75a)*

7.2.1. *Basic relations*

For mass conservation of a flame with a finite flame-front thickness τ,

$$m_o = m_u + m_b + m_f \quad (38)$$

where the subscripts u, b and f denote unburnt gas, burnt gas, and flame-front, respectively.

Hence, for mass continuity across the flame front,

$$S_t = -(1/A_u\rho_u)(\mathrm{d}m_u/\mathrm{d}t) = (1/A_u\rho_u)[(\mathrm{d}m_b/\mathrm{d}t) + (\mathrm{d}m_f/\mathrm{d}t)]. \quad (39)$$

Defining the mass-fraction "burnt and burning" as

$$n = (m_b + m_f)/m_o = 1 - (m_u/m_o) \quad (40)$$

yields

$$S_t = (m_o/A_u\rho_u)(\mathrm{d}n/\mathrm{d}t). \quad (41)$$

It is convenient for later analysis to express the variables in equations in nondimensional form using the following reference quantities:

(1) instantaneous flame-front radius, $-r_f$;
(2) vessel internal radius, $-R$;
(3) time from ignition to the flame reaching the wall, $-t_e$.

Hence

$$\tilde{\tau} = (\tau/r_f); \quad \tilde{r} = (r_f/R); \quad \tilde{t} = (t/t_e) \quad (42)$$

where the sign ˜ indicates a nondimensional quantity.

Thus, for isotropic flame propagation in a constant-volume spherical vessel:

$$m_o = (4/3)\pi R^3\rho_o \quad (43)$$

$$m_u = (4/3)\pi(R^3 - r_f^3)\bar{\rho}_u = (4/3)\pi R^3\rho_o\bar{\beta}(1 - \tilde{r}^3) \quad (44)$$

$$m_b = (4/3)\pi R^3\rho_o\tilde{r}^3\bar{\alpha}(1 - \tilde{\tau})^3 = (4/3)\pi R^3\rho_o\tilde{r}^3\bar{\alpha}F^3 \quad (45)$$

$$m_f = (4/3)\pi R^3\rho_o\tilde{r}^3\bar{\varepsilon}[1 - (1 - \tilde{\tau})^3]$$

$$= (4/3)\pi R^3 \rho_o \tilde{r}^3 \bar{\varepsilon}(1 - F^3) \quad (46)$$

$$A_u = 4\pi R^2 \tilde{r}^2 \quad (47)$$

where

$$F = (1 - \tau) \text{ and } \bar{\varepsilon} = \bar{\rho}_f/\rho_o. \quad (48)$$

Substituting the appropriate terms in eq. (41) yields

$$S_t = (R/3\tilde{r}^2\beta t_e)(\mathrm{d}n/\mathrm{d}\tilde{t}). \quad (49)$$

7.2.2. *Mass-fraction burnt and burning*

In terms of the properties of the unburnt gas

$$n_u = 1 - (m_u/m_o) = 1 - \bar{\beta} + \bar{\beta}\tilde{r}^3 \quad (50)$$

whilst in terms of the properties of the burnt and burning gases

$$n_b = (m_b/m_o) + (m_f/m_o)$$
$$= r^3[\bar{\alpha}F^3 + \bar{\varepsilon}(1 - F^3)] \quad (51)$$

or equating these to yield a combined form yields

$$n_t = (\bar{\beta} - 1)G/(\bar{\beta} - G) \quad (52)$$

where

$$G = \bar{\alpha}F^3 + \bar{\varepsilon}(1 - F^3). \quad (53)$$

7.2.3. *Laminar burning velocity equations*

Differentiating each of the expressions for mass-fraction burnt and substituting into eq. (49) in turn yields three forms of thick-flame burning velocity equation: i.e. the *unburnt gas equation*—

$$S_u = (R/t_e)(\bar{\beta}/\beta)[(\mathrm{d}\tilde{r}/\mathrm{d}\tilde{t}) - \{(1 - \tilde{r}^3)/3\tilde{r}^2\bar{\beta}\}(\mathrm{d}\bar{\beta}/\mathrm{d}\tilde{t})] \quad (54)$$

the *burnt gas equation*—

$$S_b = (R/t_e)(1/\beta)[G(\mathrm{d}\tilde{r}/\mathrm{d}\tilde{t}) + (\tilde{r}F^3/3)(\mathrm{d}\bar{\alpha}/\mathrm{d}\tilde{t}) + \{\tilde{r}(1 - F^3)/3\}(\mathrm{d}\bar{\varepsilon}/\mathrm{d}\tilde{t}) - \tilde{r}(\bar{\alpha} - \bar{\varepsilon})F^2(\mathrm{d}\bar{\tau}/\mathrm{d}\tilde{t})] \quad (55)$$

and one form of *combined equation*—

$$S_t = [\{\tilde{r}(R/t_e)(\bar{\beta}/\beta)\}/3(\bar{\beta} - G)] \times [F^3(\mathrm{d}\bar{\alpha}/\mathrm{d}\tilde{t}) + \{G(1 - G)/\beta(\bar{\beta} - 1)\}(\mathrm{d}\bar{\beta}/\mathrm{d}\tilde{t}) + (1 - F^3)(\mathrm{d}\bar{\varepsilon}/\mathrm{d}\tilde{t}) - 3(\bar{\alpha} - \bar{\varepsilon})F^2(\mathrm{d}\tilde{\tau}/\mathrm{d}\tilde{t})]. \quad (56)$$

Here again, except for very high-velocity flames it is permissible to set $\bar{\beta} = \beta = \rho_u/\rho_o$.

All the foregoing equations reduce to their corresponding thin-flame counterparts when

$$\tilde{\tau} = 0 = (\mathrm{d}\tilde{\tau}/\mathrm{d}\tilde{t}) = (\mathrm{d}\bar{\varepsilon}/\mathrm{d}\tilde{t})$$

and hence,

$$F = 1 \quad \text{and} \quad G = \bar{\alpha}.$$

7.2.4. *Corrections for flame-front thickness (GR75)*

It is generally convenient to calculate burning velocities using the thin-flame equations and then apply a correction for the effects of flame thickness.

If this correction is written in the form

$$K_c = S_t - S_t' \quad (57)$$

where S_t' is the thin-flame burning velocity, the foregoing analysis yields

$$K_c = B(\mathrm{d}r_f/\mathrm{d}t) + C(\mathrm{d}\bar{\alpha}/\mathrm{d}t) + D(\mathrm{d}\bar{\varepsilon}/\mathrm{d}t) + E(\mathrm{d}\tau/\mathrm{d}t) \quad (58)$$

where

$$B = (1/\beta)(\bar{\varepsilon} - \bar{\alpha})(1 - F^2) = E(1 - F^2)/F^2$$
$$C = -(1/\beta)(r_f/3)(1 - F^3) = -D. \quad (59)$$

A similar, but unfortunately inaccurate, equation has been derived by Andrews and Bradley (AB72).

The particular form of the thin-flame combined equation, given by eq. (33), has advantages from a data handling point of view, and is generally used to provide values of S_t' which are then corrected by the use of eq. (58).

The values of flame-front thickness, τ, and average flame-front density, $\bar{\varepsilon}$, used to correct the results of the stoichiometric methane–air tests (discussed in Section 8) were determined as follows:

(1) Assuming that $\tau \propto 1/\rho_u S_t$ was an accurate enough representation of the variation of flame thickness for methane–air, an approximate relationship for S_t in terms of p and T_u was determined from the thin-flame results, which on substitution into the above yielded

$$\tau = 1.848 \times 10^{-7}(T_o/p_o^{0.265})(p^{-1.04}) \quad (57)$$

the constant being chosen to yield $\tau = 1.1$ mm at $T_o = 300$ K and $p = p_o = 1$ atmosphere to correspond to Janisch's results (Ja71).

(2) The mean gas density ratios, $\bar{\varepsilon} = \bar{\rho}_f/\rho_o$ in the spherical shells of burning gas, were then obtained using the temperature distribution profiles of Dixon-Lewis and Wilson (DW51) by assuming that these do not vary significantly for spherical flames under the same unburnt-gas conditions, and remain similar for all flames of the same combustible mixture (GR75).

Strictly, this process of S_t correction for flame-front thickness effects should be an iterative one. However, with the present uncertainty in τ values, this does not provide reliable improvement over the currently reported data.

7.2.5. *Corroborative relations*

As with the thin-flame equations, corroborative relations are provided by the various forms of mass-fraction burnt eqs (50), (51), (52), and the burning-velocity equations (54), (55), (56). The density ratio, $\bar{\alpha}$, and maximum pressure, p_e, can be checked using eqs (34) and (35) respectively. Similar equations to those given by eqs (36) and (37) can also be derived.

8. COMPARISON OF EXPERIMENTAL RESULTS FOR STOICHIOMETRIC METHANE–AIR MIXTURES

For the purpose of comparing the experimental results of various methods used to determine burning velocity, as well as comparing these results with theoretical prediction which have recently become available (Ts78), we will confine ourselves to methane–air mixtures, and in particular to the pressure and temperature dependence of stoichiometric mixtures since these have been well reported (AB72, GR78, Ts78).

Figure 16 shows plots of burning velocity versus equivalence ratio for methane–air at $p = 1$ atmosphere (0.101 MPa) and various values of T_u as reported by different workers. Figures 17, 18 and 19 present results for stoichiometric methane–air for the ranges $0.06 \leq p \leq 2.04$ MPa and $290 \leq T_u \leq 525$ K, as obtained in a spherical constant-volume vessel (Ga75, GR78). In Fig. 17 the dependence of S_t on pressure can be seen to be initially very large at low unburnt-gas temperatures, becoming practically independent of pressure at higher pressures and temperatures. Figure 18 shows the variation of S_t with T_u for a range of pressures. Evidently, the isobars (particularly after being corrected for flame-front thickness), are essentially straight at lower pressures, and can in consequence be described by relatively simple equations, as will be discussed later. The three-dimensional representation of Fig. 19 illustrates the combined effects of both unburnt-gas temperature and pressure.

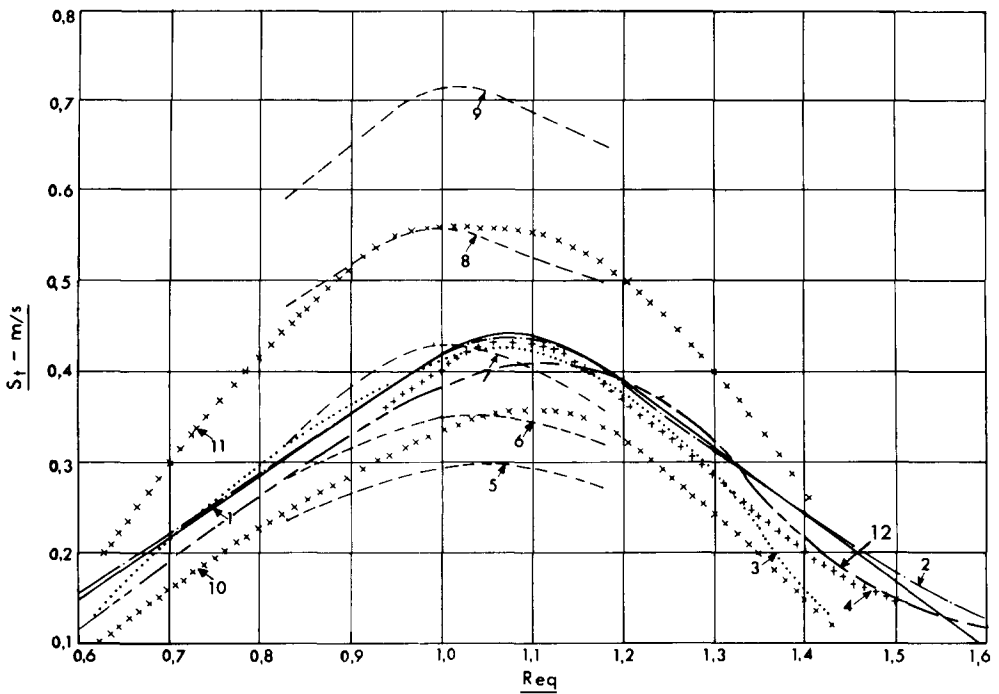

FIG. 16. Comparison of burning velocity versus equivalence ratio data for methane–air.

Curve No.	Ref.	Method	Pressure (MPa)	Temp. (K)
1	AB73	cylindrical bomb, double kernel	0.101	293
2	AB72	cylindrical bomb, hot-wire anemometer	0.101	293
3	GJ73	nozzle burner, button flame, particle tracks	0.101	293
4	RM71	nozzle burner, Schlieren cone, particle tracks	0.101	293
5				289
6		spherical bomb with heater,		313
7	BK64	Schlieren flame photography,	0.101	343
8		constant pressure region only		413
9				493
10	BK66	As for BK64	0.101	323
11				423
12	Ts78	computer prediction	0.101	298

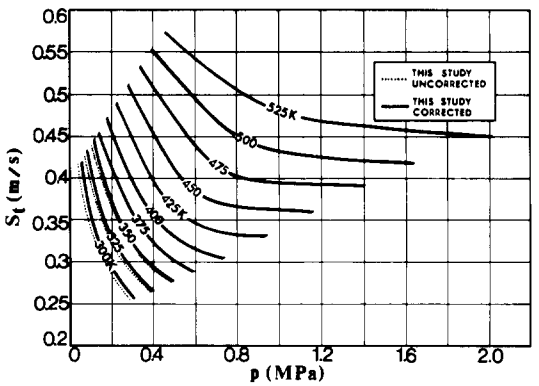

FIG. 17. Burning velocity pressure dependence for stoichiometric methane–air.

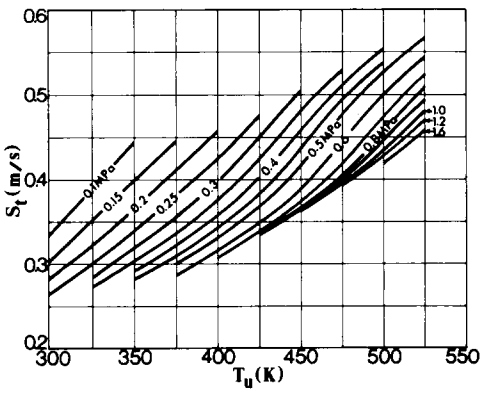

FIG. 18. Burning-velocity temperature dependence for stoichiometric methane–air.

Andrews and Bradley have, fairly recently, presented comprehensive and useful tabulations on methane–air mixtures (AB72, AB72a). It is thus unnecessary to repeat all these data here. Suffice it to say that the values of maximum burning velocities reported over the years range from as low as 0.32 m/sec to as high as 0.50 m/sec with a value, recommended by Andrews and Bradley (AB72), of 0.45 ± 0.02 m/sec at 1 atmosphere and 298 K. We believe this to be too high by about 0.08 m/sec, for reasons to be discussed in what follows.

8.1. *Equivalence Ratio*

Figure 16 gives some idea of the discrepancies which still exist between the more reliable data reported. Although there is good correspondence between the values of Andrews and Bradley (AB72, AB73), Reed *et al.* (RM71) and Gunther and Janish (GJ72), there are quite large differences between these results and those of Babkin and coworkers obtained at different times (BK64, BK66). However, recognizing that Babkin's results were determined from observations taken during the early stages of combustion in a spherical vessel, that no corrections for flame-front thickness were applied, and that simplified equations were used, we concede that their results are likely to be low—but not to the extent suggested by Andrews and Bradley.

Of considerable interest are the computer predictions published by Smoot *et al.* (SH76) and more recently by Tsatsaronis (Ts78). The latter are based on a methane–oxygen reaction mechanism consisting of 29 elementary reactions. Even though Tsatsaronis admits selecting or adjusting the chemical kinetic data to improve the agreement between calculated and measured values, his prediction, shown on Fig. 16, is about 8% below those of Andrews and Bradley (AB72, AB73) and about 3% higher than that recommended by Garforth and Rallis (GR78), all at an equivalence ratio of 1.0. This point will be taken up again elsewhere in this section. The gradual convergence of measured and predicted data is certainly a most encouraging development.

8.2. *Pressure Dependency*

Figure 17 shows a family of isotherms illustrating the pressure dependency of stoichiometric methane–air mixtures corrected for the effects of flame-front

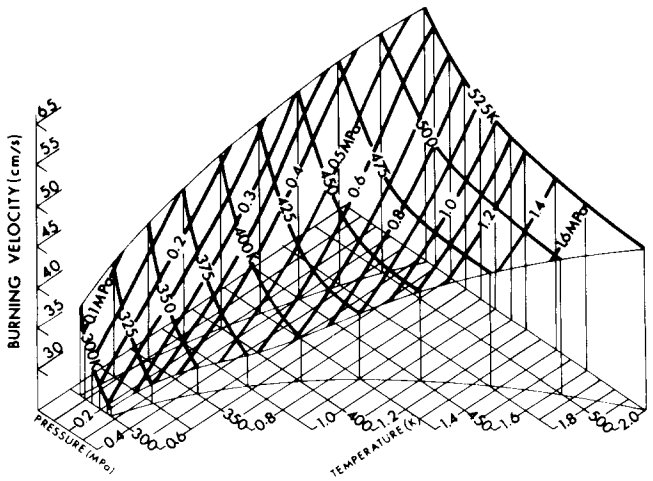

FIG. 19. Three-dimensional representation of burning velocity dependence on pressure and temperature for stoichiometric methane–air.

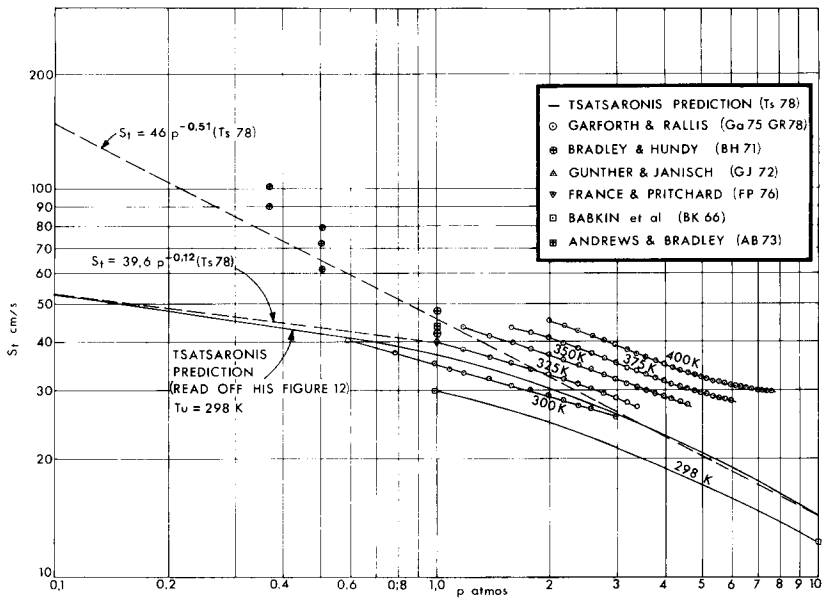

FIG. 20. Comparison of pressure dependence results for stoichiometric methane–air.

thickness (Ga75, GR78). For purposes of comparison with the results of other workers, some of these isotherms have been reproduced on a log–log plot in Fig. 20. Also included on this plot are some of the more recently published data. Of particular interest again is the plot of Tsatsaronis' predicted curve read off Fig. 12 of his paper (Ts78).

For the purpose of comparing the results obtained by various workers, consider the burning velocity at a pressure of 1 atmosphere (0.101 MPa) and an unburnt-gas temperature of 298 K. Our corrected results yield a value under these conditions of 0.353 m/sec, which we concede may be up to 5% low due to the assumption of adiabatic equilibrium flame-front temperatures. Thus, the probable value may be as high as 0.37 m/sec—essentially the value obtained by Tsatsaronis' prediction. However, the data of Bradley and Hundy, using hot-wire anemometry in closed vessel explosions (BH71); that of Andrews and Bradley from the double-kernel closed-vessel experiments (AB73); the measurements of Gunther and Janisch on button flames above a Mache–Hebra burner (GJ72); and the laser-doppler anemometer data from the nozzle-burner studies of France and Pritchard (FP76), all point to a value of S_t at 1 atmosphere and 293 K of between 0.4 and 0.5 m/sec.

For reasons discussed elsewhere (GR78) we believe that even the more reliable of these values, of just over 0.4 m/sec (GJ72, FP76), are somewhat on the high side. Certainly, however, the target range appears to be being bracketed to a value of S_t of between 0.37 and 0.4 m/sec at a pressure of 1 atmosphere and at an unburnt-gas temperature of between 293 and 298 K.

Consider next the form of the pressure dependency curves for stoichiometric methane–air mixtures. Tsatsaronis predicts a 298 K isotherm of progressively increasing negative slope with increasing pressure on a log–log plot (Fig. 20). This shows remarkable similarity with Babkin's 298 K isotherm, the absolute values of which we believe to be low. Our 300 K curve is in closer agreement numerically with Tsatsaronis', but does not "bend" to the same extent over the range $0.6 < p < 3$ atmospheres. Tsatsaronis suggests relationships of the form:

$$S_t = 46\ p^{-0.51}\ \text{(cm/sec) for } p > 4 \text{ atmospheres}$$

and

$$S_t = 39.6\ p^{-0.12}\ \text{(cm/sec) for } p < 0.6 \text{ atmospheres.}$$

Somewhat better approximations for the range 0.1–10 atmospheres would appear to result from:

$$S_t = 38\ p^{-0.145}\ \text{(cm/sec) for } p < 0.6 \text{ atmospheres}$$

$$S_t = 36\ p^{-0.265}\ \text{(cm/sec) for } 0.6 < p < 3 \text{ atmospheres}$$

and

$$S_t = 46\ p^{-0.51}\ \text{(cm/sec) for } 3 < p < 10 \text{ atmospheres.}$$

In the light of the foregoing, the values reported by Bradley *et al.* at pressures below 1 atmosphere must be considered too high, since they do not follow what are considered to be more reliable trends.

Still on the subject of trends, it will be noted from Figs 17 and 20 that according to our results, pressure dependency appears to diminish at higher pressures and temperatures, as shown by a flattening off of the higher temperature isotherms at higher pressures. This is in conflict both with Babkin's results and Tsatsaronis' prediction. No obvious reasons for these anomalies come to mind at present and their elucidation will have to await further work.

8.3. *Temperature Dependency*

Figure 18 shows isobars (uncorrected for flame-front thickness) of S_t versus T_u (Ga75, GR78). Again, for purposes of comparison with the results of other

workers, some of these corrected isobars have been replotted on a log–log basis in Fig. 21.

With the exception of the isobars lying in the region T_u higher than about 430 K, the nature of the temperature dependence curves appears to be less complex than their pressure counterparts. Thus, at temperatures below about 430 K they reduce to straight but slightly divergent lines, which are approximately described by an equation of the form $S_t = cT_u^d$, the constants c and d having the values given on Fig. 21.

Evidently, empirical curve fitting to data such as that depicted on Fig. 21 is a relatively arbitrary process when applied to the limited range of data available. Thus, e.g., our measured 0.1 MPa (0.99 atmospheres) isobar can be made to coincide with Tsatsaronis' curve by plotting values of $(S_t - 7)$ rather than $(S_t - 10)$ cm/sec. Until reliable theoretical reasons for using a particular exponent for T_u are proposed (such as the detailed reaction schemes of Smoot *et al.* and Tsatsaronis), it is perhaps advisable to confine oneself in any application context to the use of reliable experimental data.

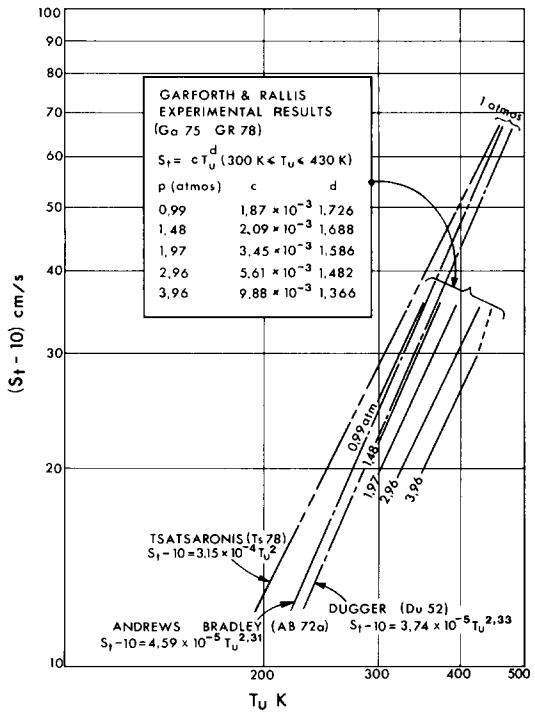

FIG. 21. Comparison of temperature dependence results for stoichiometric methane–air.

9. SUMMARY AND CONCLUSIONS

The various methods which have been used for the experimental determination of laminar burning velocity have been reviewed. Available results from some of the more recent experiments on methane–air mixtures have been compared both against each other and against computer predictions which have recently become available (Ts78). These indicate a progressive narrowing of the bounds of uncertainty and suggest a benchmark value of $S_t = 0.37 \pm 0.02$ m/sec for stoichiometric methane–air at $p = 1$ atmosphere and $T_u = 298$ K. The position regarding the pressure and temperature dependency of burning velocity for this mixture is evidently relatively complex and requires further investigation both from the theoretical and experimental viewpoints. However, because of the compatibility of the computer predicted trends and those obtained by bomb methods, it is possible to propose limited empirical correlation equations over limited ranges of T_u and p.

The conclusion is reached that of the experimental methods involving stationary flames, nozzle-burner methods with either optical or laser-doppler particle-tracking techniques appear most effective—provided unburnt-gas temperatures can be accurately monitored. Alternatively, inverted-cone burners with the same measuring techniques might be worth investigating.

Of the propagating flame methods, there seems little doubt that the constant-volume vessel technique is the most versatile and accurate. Also, by using its self-corroborative characteristics, its computational complexity can be considerably reduced.

Acknowledgement—This work has been partially sponsored over the years by the South African Council for Scientific and Industrial Research, to whom the authors express their appreciation.

REFERENCES

(AB72) ANDREWS, G. E. and BRADLEY, D. Determination of burning velocities: a critical review, *Combust. Flame* **18**, 133–153 (1972).

(AB72a) ANDREWS, G. E. and BRADLEY, D. The burning velocity of methane/air mixtures, *Combust. Flame* **19**, 275–288 (1972).

(AB73) ANDREWS, G. E. and BRADLEY, D. Determination of burning velocity by double ignition in a closed vessel, *Combust. Flame* **20**, 77–89 (1973).

(AC60) ADAMS, G. R. and COOK, G. B. The effect of pressure on the mechanism and speed of the hydrazine decomposition flame, *Combust. Flame* **4**, 9–18 (1960).

(AF49) ANDERSON, J. W. and FEIN, R. S. Measurements of normal burning velocities and flame temperatures of Bunsen flames, *J. Chem. Phys.* **17**, 1268–1273 (1949).

(AF50) ANDERSON, J. W. and FEIN, R. S. Measurement of normal burning velocities of propane/air flames from shadow photographs, *J. Chem. Phys.* **19**, 441–443 (1950).

(AG61) AGNEW, J. T. and GRAIFF, L. B. The pressure dependence of laminar burning velocity by the spherical bomb method, *Combust. Flame* **5**, 209–219 (1961).

(BB55) BOLZ, R. E. and BURLAGE, H. *Jet Propulsion* **25**, 265 (1955).

(BB60) BOLZ, R. E. and BURLAGE, H. Propagation of free flames in laminar and turbulent flow fields, *NASA Tech. Note D*-551 (1960).

(BH71) BRADLEY, D. and HUNDY, G. F. Burning velocities of methane/air mixtures using hot-wire anemometers in closed vessel explosions, *Thirteenth Symp. (Int.) on Combustion*, pp. 575–581, The Combustion Institute, Pittsburgh (1971).

(BK62) BABKIN, V. S., KUZNETSOV, I. L. and KOZANCHENKO, L. S. Influence of curvature on the rate of propagation of a laminar flame in a lean

propane/air mixture. *Dokl. Akad. Sci. SSSR* **146**, (3) 625–627 September (1962); English translation, *Proc. Acad. Sci. USSR*, Phys. Chem. Soc. **146**, 677–679 (1962).

(BK64) BABKIN, V. S., KOZACHENKO, L. S. and KUZNETSOV, I. L. The influence of pressure on the burning velocity of methane/air mixtures. *Zh. Prike Mekhan. Tekn. Fiz.* 145–149 (1964).

(BK65) BABKIN, V. S. and KOZACHENKO, L. S. Energy losses in explosions in a sphere. *Fiz. Goren Vzryva* **1** (2) 114–117 (1965); English translation, *Combustion, Explosion and Shock Waves* **1**, 81–83 (1965).

(BK66) BABKIN, V. S. and KOZACHENKO, L. S. Study of normal burning velocity in methane/air mixtures at high pressures. *Fiz. Goren Vzryva* **2** (3) 77–86 (1966); English translation, *Combustion, Explosion and Shock Waves* **2**, 46–52 (1966).

(BK67) BABKIN, V. S. and KONONENKO, V. G. Equations for the determination of burning velocity in a spherical constant volume bomb. *Fiz. Goren Vzryva* **3** (2) 268–275 (1967).

(Bl73) BLEDJIAN, L. Computation of time-dependent laminar flame structure. *Combust. Flame* **20**, 5–17 (1973).

(Br49) BROEZE, J. *Third Symp. on Combustion*, p. 146, Williams and Wilkins, Baltimore (1949).

(BS54) BOTHA, J. P. and SPALDING, D. B. The laminar flame speed of propane/air mixtures with heat extraction from the flame. *Proc. Roy. Soc.* **A225**, 71–96 (1954).

(BS57) BOLLINGER, L. E., STRAUSS, W. A. and EDSE, R. *Ind. engng Chem.* **49**, 768 (1957).

(BS69) BALIN, V. A., SHORIN, S. N. and ERMOLAEV, O. N. *Teploenergetika* **16**, 75 (1969); English translation, *Thermal Engng* **4**, 109 (1969).

(BT27) BONE, W. A. and TOWNEND, D. T. A. *Flame and Combustion in Gases*, Chapters 11–14, Longmans, London (1927).

(BV66) BABKIN, V. S., V'YUN, A. V. and KOZACHENKO, L. S. The effect of pressure on normal flame velocity investigated by the initial-section method in a constant volume vessel. *Fiz. Goren Vzryva* **2** (2) 52–60 (1966); English translation, *Combustion, Explosion and Shock Waves* **2** (2) 32–37, April (1966).

(BW53) BURGOYNE, J. H. and WEINBERG, F. A method of analysis of a plane combustion wave, *Fourth Symp. on Combustion*, pp. 294–302, Williams and Wilkins, Baltimore (1953).

(BW54) BURGOYNE, J. H. and WEINBERG, F. *Proc. Roy. Soc.* **A224**, 216–308 (1954).

(CH32) COWARD, H. F. and HARTWELL, F. J. Studies in the mechanism of flame movement. Part I: The uniform movement of flame in mixtures of methane and air, in relation to tube diameter. *J. Chem. Soc. (London)* 1996–2004 (1932); Part II: The fundamental speed in mixtures of methane and air, *ibid*, pp. 2676–2684.

(CH63) CAMPBELL, E. S., HEINEN, F. J. and SCHALIT, L. M. A theoretical study of some properties of laminar steady state flames as a function of properties of their chemical components. *Ninth (Int.) Symp. on Combustion*, pp. 72–80, Academic Press (1963).

(CK55) CALCOTE, H. F. and KING, I. R. Studies of ionization in flames by means of Langmuir probes. *Fifth (Int.) Symp. on Combustion*, pp. 423–434, Reinhold, New York (1955).

(CL51) CONAN, H. R. and LINNETT, J. W. Burning velocity determination. Part V—The use of Schlieren photography in determining burning velocities by the burner method, *Trans. Faraday Soc.* **47**, 981–988 (1951).

(CL59) COMBOURIEU, J. and LAFFITTE, P. *Compt. Rendus* **248**, 802 (1959).

(Co62) COMBUOURIEU, J. Méthodes de la bombe sphérique et du tube. Revue générale des résultants. *Experimental Methods in Combustion Research* (Ed. SURUGUE, J.) Section 1.3, *Flame propagation velocity*, pp. 25–55, AGARD. Pergamon Press, London (1962).

(CP37) COWARD, H. F. and PAYMAN, W. *Chem. Rev.* **21**, 359 (1937).

(CW63) CHASE, J. D. and WEINBERG, F. J. *Proc. Roy. Soc.* **A275**, 411 (1963).

(De49) DERY, R. J. *Third Symp. on Combustion and Flame and Explosion Phenomena*, p. 235, Williams and Wilkins, Baltimore (1949).

(Di53) DIXON-LEWIS, G. Temperature distribution in flame reaction zones, *Fourth Symp. on Combustion*, pp. 263–267, Williams and Wilkins, Baltimore (1953).

(Di67) DIXON-LEWIS, G. Flame structure and flame reaction kinetics. I. Solution of conservation equations and application to rich hydrogen-oxygen flames. *Proc. Roy. Soc.* **A298**, 495–513 (1967).

(DG75) DIXON-LEWIS, G., GOLDSWORTHY, F. A. and GREENBERG, J. B. Flame structure and flame reaction kinetics. IX. Calculation of properties of multiradical premixed flames. *Proc. Roy. Soc.* **A346**, 261–278 (1975).

(DS57) DUGGER, G. L., SIMON, D. M. and GERSTEIN, M. Laminar flame propagation, Chapter IV. Basic considerations in the combustion of hydrocarbon fuels with air. *NACA Report* 1300, p. 127 (1957).

(DS74) DIXON-LEWIS, G. and SHEPHERD, I. G. Some aspects of ignition by localized sources and of cylindrical and spherical flames. *Fifteenth (Int.) Symp. on Combustion*, pp. 1483–1491, The Combustion Institute, Pittsburgh (1974).

(Du52) DUGGER, G. L. Effect of initial temperature on flame speed of methane–air, propane–air and ethylene–air mixtures. *NACA Report* 1061 (1952).

(DW51) DIXON-LEWIS, G. and WILSON, M. J. G. A method for the measurement of the temperature distribution in the inner cone of a Bunsen flame, *Trans. Faraday Soc.* **47**, 1106–1114 (1951).

(DW67) DIXON-LEWIS, G. AND WILLIAMS, A. Some observations on the combustion of methane in premixed flames, *Eleventh (Int.) Symp. on Combustion*, pp. 951–958, The Combustion Institute, Pittsburgh (1967).

(EA58) ESCHENBACH, R. C. and AGNEW, J. T. Use of the constant volume bomb technique for measuring burning velocity, *Combust. Flame* **2** (3) 273–285 (1958).

(EH69) EDMONDSON, H. and HEAP, M. P. The burning velocity of methane/air flames inhibited by methyl bromide, *Combust. Flame* **13**, 472–478 (1969).

(EH70) EDMONDSON, H. and HEAP, M. P. *Combust. Flame* **14**, 195 (1970).

(El28) ELLIS, O. C. Flame movement in gaseous explosive mixtures, *Fuel* **7**, 245 (1928).

(Es57) ESCHENBACH, R. C. Use of the constant volume bomb technique for measuring burning velocities. Ph.D. Thesis, Purdue University, Indiana (1957).

(ET52) EGERTON, A. C. and THABET, S. K. Flame propagation: the measurement of burning velocities of slow flames and the determination of the limits of combustion, *Proc. Roy. Soc.* **211A**, 445–471 (1952).

(EW27) ELLIS, O. C. and WHEELER, R. V. The movement of flame in closed vessels: after-burning, *J. Chem. Soc. pp.* 310–322 (1927).

(FA54) FRISTROM, R. M., AVERY, W. H., PRESCOTT, R. and MATTUCK, A. Flame zone studies by the particle track technique. I. Apparatus and technique. *J. Chem. Phys.* **22**, 106–109 (1954).

(FB54) FRIEDMAN, R. and BURKE, E. Measurement of temperature distribution in low-pressure flat flame, *J. Chem. Phys.* **22**, 824–830 (1954).

(Fi43) FIOCK, E. F. A survey of combustion research in *The Chemical Background for Engine Research*, (Eds BURK, R. E. and GRUMMITT, O.) *Frontiers in Chemistry*, Vol. II, pp. 1–53, Interscience Publishers, New York (1943).

(Fi55) FIOCK, E. F. Physical measurements in gas dynamics and combustion, *High Speed Aerodynamics and Jet Propulsion*, Vol. 9, p. 409, Oxford University Press, London (1955).

(FK35) FIOCK, E. F. and KING, H. K. The effect of water vapour on flame velocity in equivalent CO–O_2 mixtures, *NACA Report* 531 (1935).

(FM17) FLAMM, L. and MACHE, H. *Wien Ber* **9**, 126 (1917) (Cited by LV51, p. 451); MACHE, H. *Die Physik der Verbrennungserscheinunge*, Veit and Co. Leipzig, (1918) (Cited by LV51, p. 249).

(FM37) FIOCK, E. F. and MARVIN, C. F. The measurement of flame speed. *Chem. Rev.* **21** (3), 367–387 (1937).

(FM40) FIOCK, E. F., MARVIN, C. F., CALDWELL, F. R. and ROEDER, C. H. Flame speeds and energy considerations for explosions in a spherical bomb, *NACA Report* 682 (1940).

(FP69) FULLER, L. E., PARKS, D. J. and FLETCHER, E. A. *Combust. Flame* **13**, 455 (1969).

(FP76) FRANCE, D. H. and PRITCHARD, R. Laminar burning velocity measurements using a laser-doppler anemometer, *J. Inst. Fuel* **79**, 78–82 (1976).

(FR35) FIOCK, E. F. and ROEDER, C. H. The soap bubble method of studying the combustion of mixtures of CO and O_2, *NACA Report* 532 (1935); *ibid.* Some effects of argon and helium upon explosions of carbon monoxide and oxygen, *NACA Report* 553 (1936).

(Fr53) FRIEDMAN, R. Measurement of the temperature profile in a laminar flame. *Fourth Symp. on Combustion*, pp. 259–263, Williams and Wilkins, Baltimore (1953).

(Fr56) FRISTROM, R. M. Flame zone studies. II. Applicability of one-dimensional models to three-dimensional laminar Bunsen flame fronts, *J. Chem. Phys.* **24**, 888–894 (1956).

(Fr57) FRISTROM, R. M. The structure of laminar flames. *Sixth (Int.) Symp. on Combustion*, pp. 96–110, Reinhold, New York (1957).

(Fr61) FRISTROM, R. M. Experimental determination of local concentrations in flames, *Experimental Methods in Combustion Research* (Ed. SURUGUE, J.) Section 1.4, AGARD. Pergamon Press, London (1961).

(Fr65) FRISTROM, R. M. Definition of burning velocity and a geometric interpretation of the effects of flame curvature. *Phys. of Fluids* **8** (2), 273–280 (1965).

(FW65) FRISTROM, R. M. and WESTENBERG, A. A. *Flame Structure*, McGraw-Hill Book Co. New York (1965).

(Ga73) GARFORTH, A. M. A computer programme for the calculation of equilibrium composition and adiabatic flame temperatures of gaseous mixtures undergoing constant pressure combustion. University of the Witwatersrand, School of Mechanical Engineering, *Research Report No.* 56, August (1973).

(Ga74) GARFORTH, A. M. Measurement of rapidly varying density, and hence temperature, by laser interferometry in the unburnt gas region of a spherical constant volume vessel during flame propagation. University of the Witwatersrand, School of Mechanical Engineering, *Research Report No.* 57, August (1974).

(Ga75) GARFORTH, A. M. Theoretical and experimental development of the constant volume method for determining laminar burning velocity, Ph.D. Thesis, University of the Witwatersrand, February (1975).

(Ga76) GARFORTH, A. M. Unburnt gas density measurement in a spherical combustion bomb by infinite-fringe laser interferometry, *Combust. Flame* **26**, 343–352 (1976).

(GC59) GRUMER, J., COOK, E. B. and KUBALA, T. A. Considerations pertaining to spherical-vessel combustion, *Combust. Flame* **3** (4), 437–446 (1959).

(Ge53) GERSTEIN, M. The structure of laminar flames. *Fourth (Int.) Symp. on Combustion*, pp. 35–43, Williams and Wilkins, Baltimore (1953).

(GH50) GROVE, J. R., HOARE, M. F. and LINNETT, J. W. The shadow cast by a Bunsen flame, its production and usefulness, *Trans. Faraday Soc.* **46**, 745–755 (1950).

(Gi57) GILBERT, M. The influence of pressure on flame speed, *Sixth (Int.) Symp. on Combustion*, pp. 74–83, Reinhold, New York (1957).

(GJ72) GÜNTHER, R. and JANISCH, B. Measurement of burning velocity in a flat flame front, *Combust. Flame* **19**, 49–53 (1972).

(GL49) GARNER, F. H., LONG, R. and ASHFORTH, G. R. Determination of burning velocities in benzene–air mixtures. *Fuel* **28** (12), 272–276 (1949).

(GL51) GERSTEIN, M., LEVINE, O. and WONG, E. L. Flame propagation. II. The determination of fundamental burning velocities of hydrocarbons by a revised tube method, *J. Am. Chem. Soc.* **73**, 418–422 (1951).

(GL53) GILBERT, M. and LOBDELL, J. H. Resistance-thermometer measurements in a low-pressure flame, *Fourth (Int.) Symp. on Combustion*, pp. 285–294, Williams and Wilkins, Baltimore (1953).

(GM48) GUENOCHE, H., MANSON, N. and MONNET, G. La propagation uniforme d'une déflagration dans un tube cylindrique lisse. *CR Acad. Sci. Paris*, **226**, 163–164 (1948); L'influence des conditions aux limits longitudinales sur la propagation des déflagrations dans les tubes cylindrique lisses. *CR. Acad. Sci. Paris*, **226**, 69–71 (1948).

(Go76) GOULARD, R. (Ed.) *Combustion Measurements*. Academic Press, New York (1976).

(Gr59) GRAIFF, L. B. The pressure dependence of laminar burning velocity. Ph.D. Thesis, Purdue University, Indiana (1959).

(GR75) GARFORTH, A. M. and RALLIS, C. J. The spherical bomb method for laminar burning velocity determination: Equations for thick flame propagation. University of the Witwatersrand, School of Mechanical Engineering, *Research Report No.* 59 (1975); Also presented at *The Second European Symp. on Combustion*, Orleans, France, September (1975).

(GR75a) GARFORTH, A. M. and RALLIS, C. J. Analysis of gas movement during flame propagation, University of the Witwatersrand, School of Mechanical Engineering, *Research Report No.* 64 (1975); Also presented at *The Fifth Int. Colloquium on Gas Dynamics of Explosions and Reactive Systems*, Bourges, France, September (1975).

(GR76) GARFORTH, A. M. and RALLIS, C. J. Equipment, experimental procedure and data handling, University of the Witwatersrand, School of Mechanical Engineering, *Research Report No.* 65 (1976).

(GR78) GARFORTH, A. M. and RALLIS, C. J. Laminar burning velocity of stoichiometric methane–air: pressure and temperature dependence. *Combust. Flame* **31**, 53–68 (1978).

(GW53) GAYDON, A. G. and WOLFAARD, H. G. *Flames. Their Structure, Radiation and Temperature*, Chapman and Hall, London (1953).

(GW60) *ibid.* 2nd revised edition (1960).

(GW70) *ibid.* 3rd revised edition (1970).

(HC53) HIRSCHFELDER, J. O., CURTISS, C. F. and CAMPBELL, D. E. The theory of flame propagation IV. *J. Chem. Phys.* **57**, 403–414 (1953).

(HC54) HIRSCHFELDER, J. D., CURTISS, C. F. and BIRD, R. B. *Molecular Theory of Gases and Liquids*. John Wiley, New York (1954).

(HH56) HENDERSON, H. T. and HILL, G. R. *J. Phys. Chem.* **60**, 874 (1956).

(HK77) HALSTEAD, M. P., KIRSCH, L. J. and QUINN, C. P. The autoignition of hydrocarbon fuels at high temperatures and pressures—Fitting of a mathematical model, *Combust. Flame* **30**, 45–60 (1977).

(Ho06) HOPKINSON, B. Explosions of coal-gas and air, *Proc. Roy. Soc.* **A77**, 387–413 (1906).

(Ja71) JANISCH, G. *Chem. Ing. Techn.* **43**, 561 (1971).

(Jo46) JOST, W. *Explosion and Combustion Processes in Gases*, (translated by CROFT, H. O.) McGraw-Hill, New York (1946).

(Ke68) KELLER, H. B. *Numerical Methods for Two-Point Boundary-Value Problems*, Blaisdell-Ginn, Waltham, Massachusetts (1968).

(KN59) KINBARA, T., NAKAMURA, J. and IKEGAMI, H. Distribution of ions in low-pressure flames, *Seventh (Int.) on Combustion*, pp. 263–268, Butterworths, London (1959).

(KU62) KIMURA, I. and UKAWA, H. *Eighth Symp. (Int.) on Combustion*, p. 521, Williams and Wilkins (1962).

(KW48) KLAUKENS, H. and WOLFHARD, H. G. Measurements in the reaction zone of a Bunsen flame, *Proc. Roy. Soc.* **A193**, 512–524 (1948).

(La62) LAFFITTE, P. Méthodes du brûleur et de la butte de savan, *Experimental Methods in Combustion Research* (Ed. SURUGUE, J.), Section 1.3, *Flame propagation velocity*, pp. 4–24, AGARD. Pergamon Press, London (1962).

(LC64) LAFFITTE, P. and COMBOURIEU, J. *Journées Internationales de la Combustion et de la Conversion de l'Énergie*, p. 55, Institut Français des Combustibles et de l'Énergie, Paris (1964) (Cited by AB72).

(Le54) LEWIS, B. *Selected Combustion Problems*, discussion, pp. 176–179, AGARD, Butterworths, London (1954).

(Le59) LEWIS, B. Remarks on combustion science, *Seventh (Int.) Symp. on Combustion*, pp. xxxi–xxxv, Butterworths, London (1959).

(Li53) LINNETT, J. W. Methods of measuring burning velocities, *Fourth (Int.) Symp. on Combustion*, pp. 20–35, Williams and Wilkins, Baltimore (1953).

(Li54) LINNETT, J. W. Some experimental results relating to laminar flame propagation, *Selected Combustion Problems*, pp. 92–110, AGARD. Butterworths, London (1954).

(Li67) LINDOW, R. *Gas Wärme Int.* **16**, 405 (1967).

(Li67a) LINDOW, R. *Gas and Wasserfach*, **108**, 573 (1967) (Cited by AB72).

(Li68) LINDOW, R. *Brennstoff Wärme Kraft* **20**, 8 (1968) (Cited by AB72).

(LP51) LINNETT, J. W., PICKERING, H. S. and WHEATLEY, P. J. Burning velocity determinations. Part IV—The soap bubble method of determining velocities. *Trans. Faraday Soc.* **47**, 974–980 (1951).

(LV34) LEWIS, B. and VON ELBE, G. Determination of the speed of flames and the temperature distribution in a spherical bomb from time pressure records. *J. Chem. Phys.* **2**, 283–290 (1934).

(LV51) LEWIS, B. and VON ELBE, G. *Combustion Flames and Explosions of Gases*, Academic Press, New York (1951).

(LV56) LEWIS, B. and VON ELBE, G. Combustion waves in non-turbulent explosive gas, *High Speed Aerodynamics and Jet Propulsion Series*, Vol. II, *Combustion Processes*, Section G, pp. 216–231, Oxford University Press, London (1956).

(LV61) LEWIS, B. and VON ELBE, G. *Combustion Flames and Explosions of Gases*, 2nd Edition, Academic Press, New York (1961).

(LW59) LEVY, A. and WEINBERG, F. J. Optical flame structure studies: some conclusions concerning the propagation of flat flames, *Seventh (Int.) Symp. on Combustion*, pp. 296–303, Butterworths, London (1959).

(ML53) MELLISH, C. F. and LINNETT, J. W. The influence of inert gases on some flame phenomena, *Fourth (Int.) Symp. on Combustion*, pp. 407–420, Williams and Wilkins, Baltimore (1953).

(MV53) MANTON, J., VON ELBE, G. and LEWIS, B. Burning velocity measurements in a spherical vessel with central ignition, *Fourth (Int.) Symp. on Combustion*, pp. 358–363, Williams and Wilkins, Baltimore (1953).

(Na07) NAGEL, A. *Farschungsh Ver dtsch Ing* **54** (1907); *Engineering* (London) **86**, 278 (1908) (Cited by St26).

(Ol49) OLSEN, H. L. Interferometric methods, *Third Symp. on Combustion*, pp. 663–667, Williams and Wilkins, Baltimore (1949).

(OR59) O'DONOVAN, K. H. and RALLIS, C. J. A modified analysis for the determination of the burning velocity of a gas mixture in a spherical constant volume combustion vessel, *Combust. Flame* **5** (**2**), 201–214 (1959).

(PB59) PONCELET, J., BERENDSEN, R. and VAN TIGGELEN, A. Comparative study of ionization in acetylene–oxygen and acetylene–nitrous oxide flames, *Seventh (Int.) Symp. on Combustion*, pp. 256–262, Butterworths, London (1959).

(PD66) PENZIAS, G. J., DOLIN, S. A. and KRUEGLE, H. A. Spectroradiometric pyrometry of shock-heated gases by infrared emission and absorption measurements, *App. Opt.* **5**, 225–230 (1966).

(PL51) PICKERING, H. S. and LINNETT, J. W. Burning velocity determination. Part VI. The use of Schlieren photography in determining burning velocities by the soap bubble method, *Trans. Faraday Soc.* **17**, 989–992 (1951).

(Po49) POWLING, J. A new burner method for the determination of low burning velocities and limits of inflammability, *Fuel* (London) **28**, 25–28 (1949).

(Po61) POWLING, J. The flat flame burner, *Experimental Methods in Combustion Research* (Ed. SURUGUE, J.) Section 2.2.1, AGARD. Pergamon Press, London (1961).

(PP53) PRICE, T. W. and POTTER, J. H. Factors affecting flame velocity in stoichiometric carbon monoxide oxygen mixtures, *Fourth (Int.) Symp. on Combustion*, pp. 363–369, Williams and Wilkins, Baltimore (1953).

(Ra59) RALLIS, C. J. Mean temperature of burnt gases, *Combust. Flame* **3** (**3**), 419–420 (1959).

(Ra63) RALLIS, C. J. A critical evaluation of the spherical constant volume vessel method for determining laminar burning velocity, Ph.D. Thesis, University of the Witwatersrand, Johannesburg, August (1963).

(Ra64) RALLIS, C. J. The determination of laminar burning velocity with particular reference to the constant volume method. Part I—Theory. University of the Witwatersrand, Dept. of Mechanical Engineering, *Research Report No.* 20 (1964).

(RG65) RALLIS, C. J., GARFORTH, A. M. and STEINZ, J. A. Laminar burning velocity of acetylene/air mixtures by the constant volume method: dependence on mixture composition, pressure and temperature, *Combust. Flame* **9**, 345–356 (1965).

(RG65a) RALLIS, C. J., GARFORTH, A. M. and STEINZ, J. A. The determination of laminar burning velocity with particular reference to the constant volume method. Part 2—Apparatus. University of the Witwatersrand, Dept. of Mechanical Engineering, *Research Report No.* 25 (1965).

(RG65b) *ibid.* Part 3—Experimental procedure and results, *Research Report No.* 26 (1965).

(RM71) REED, S. B., MINEUR, J. and MCNAUCHTON, J. P. The effect on the burning velocity of methane of vitiation of combustion air, *J. Inst. Fuel* **44**, 149–155 (1971).

(RO62) RAEZER, S. D. and OLSEN, H. L. Measurement of laminar flame speeds of ethylene–air and propane–air mixtures by the double kernel method, *Combust. Flame* **6**, 227–232 (1962).

(RP62) RALLIS, C. J., POSEL, K. and TREMEER, G. E. B. The determination of burning velocities of normal combustion flames in a spherical constant volume vessel, *S.A. mech. Engineer*, **11** (**8**), 233–255 (1962).

(RT63) RALLIS, C. J. and TREMEER, G. E. B. Equations for the determination of burning velocity in a spherical constant volume vessel, *Combust. Flame* **7** (**1**), 51–61 (1963).

(SA57) SMITH, D. and AGNEW, J. T. The effect of pressure on the laminar burning velocity of methane–oxygen–nitrogen mixtures, *Sixth (Int.) Symp. on Combustion*, pp. 83–88, Reinhold, New York (1957).

(SE59) STRAUSS, W. A. and EDSE, R. Burning velocity measurements by the constant-pressure bomb method, *Seventh (Int.) Symp. on Combustion*, pp. 377–385, Butterworths, London (1959).

(Se61) SENIOR, D. A. Burning velocities of hydrogen–air and hydrogen–oxygen mixtures. Determination by burner method with Schlieren photography. *Combust. Flame* **5** (**1**), 7–10 (1961).

(SG56) SINGER, J. M., GRUMER, J. and COOK, E. B. *Proc. Gas Dynamics Symp. on Aerothermochemistry*, p. 139, Northwestern University, Evanston, Illinois (1956).

(Sh73) SHIMIZU, S. Temperature measurement of premixed fuel–air mixtures by an infrared radiation pyrometer, *Bull. JSME* **16** (**92**), 333–344 (1973).

(SH76) SMOOT, L. D., HECKER, W. C. and WILLIAMS, G. A. Prediction of propagating methane–air flames, *Combust. Flame* **26**, 323–342 (1976).

(Si59) SIMON, D. M. *Seventh (Int.) Symp. on Combustion*, Discussion p. 413, Butterworths, London (1959).

(SL48) SHERRAT, S. and LINNETT, J. W. The determination of flame speeds in gaseous mixtures, *Trans. Faraday Soc.* **44**, 596–608 (1948).

(Sm37) SMITH, F. A. Problems of stationary flames, *Chem. Rev.* **21** (**21**), 389–412 (1937).

(Sp56) SPALDING, D. B. The theory of flame phenomena with a chain reaction, *Phil. Trans. Roy. Soc.* (London) **A249**, 1–25 (1956).

(Sp57) SPALDING, D. B. Predicting the laminar flame speed in gases with temperature-explicit reaction rates, *Combust. Flame* **1**, 287–295 (1957).

(SS53) STREHLOW, R. A. and STUART, J. G. An improved soap bubble method of measuring flame velocities, *Fourth (Int.) Symp. on Combustion*, pp. 329–336, Williams and Wilkins, Baltimore (1953).

(SS71) SPALDING, D. B., STEPHENSON, P. L. and TAYLOR, R. G. A calculation procedure for the prediction of laminar flame speeds, *Combust. Flame* **17**, 55–64 (1971).

(St23) STEVENS, F. W. *NACA Reports*, 176 (1923); 280 (1927); 305 (1929); 337 (1929); 372 (1930).

(St26) STEVENS, F. W. The rate of flame propagation in gaseous explosive reactions, *J. Am. Chem. Soc.* **48**, 1896 (1926); *ibid.* **50**, 3244 (1928).

(SW53) SIMON, D. and WONG, E. L. Burning velocity measurements, *J. Chem. Phys.* **21**, 936 (1953).

(SW54) SIMON, D. M. and WONG, E. L. An evaluation of the soap bubble method for burning velocity measurements using ethylene–oxygen–nitrogen and methane–oxygen–nitrogen mixtures, *NACA Tech. Note* 3106, February (1954).

(Tr62) TREMEER, G. E. B. The determination of the burning velocities of gaseous mixtures using a spherical constant volume combustion vessel, M.Sc. Thesis, University of the Witwatersrand, Johannesburg, August (1962).

(Ts78) TSATSARONIS, G. Prediction of propagating laminar flames in methane, oxygen, nitrogen mixtures, *Combust. Flame* **33**, 217–239 (1978).

(VK74) VANCE, G. M. and KRIER, H. A theory for spherical and cylindrical laminar premixed flames, *Combust. Flame* **22**, 365–375 (1974).

(VL43) VON ELBE, G. and LEWIS, B. Stability and structure of burner flames, *J. Chem. Phys.* **11**, 75–97 (1943).

(WF61) WESTENBERG, A. A. and FRISTROM, R. M. Methane–oxygen flame structure. IV. Chemical kinetic considerations. *J. Phys. Chem.* **65**, 591 (1961).

(Wo49) WOHL, K. *Third Symp. on Combustion*, p. 203, Williams and Wilkins, Baltimore (1949).

(ZB59) ZELDOVICH, Y. B. and BARENBLATT, G. I. Theory of flame propagation, *Combust. Flame* **3**, 61–74 (1959).

(*Manuscript received* 8 *February* 1980)